



**HAL**  
open science

## Environmental Analogs from Yellowstone hot springs on Geochemical and Microbial Diversity with Implications for the Search for Life on Mars

D Boulesteix, A Buch, G Masson, L L Kivrak, J R Havig, T L Hamilton, B L Teece, Y He, Caroline Freissinet, Y Huang, et al.

### ► To cite this version:

D Boulesteix, A Buch, G Masson, L L Kivrak, J R Havig, et al.. Environmental Analogs from Yellowstone hot springs on Geochemical and Microbial Diversity with Implications for the Search for Life on Mars. Planetary and Space Science, inPress, 10.1016/j.pss.2024.105953 . insu-04672206v1

**HAL Id: insu-04672206**

**<https://insu.hal.science/insu-04672206v1>**

Submitted on 17 Aug 2024 (v1), last revised 13 Sep 2024 (v2)

**HAL** is a multi-disciplinary open access archive for the deposit and dissemination of scientific research documents, whether they are published or not. The documents may come from teaching and research institutions in France or abroad, or from public or private research centers.

L'archive ouverte pluridisciplinaire **HAL**, est destinée au dépôt et à la diffusion de documents scientifiques de niveau recherche, publiés ou non, émanant des établissements d'enseignement et de recherche français ou étrangers, des laboratoires publics ou privés.



Distributed under a Creative Commons Attribution 4.0 International License

# Journal Pre-proof



Environmental Analogs from Yellowstone hot springs on Geochemical and Microbial Diversity with Implications for the Search for Life on Mars

D. Boulesteix, A. Buch, G. Masson, L.L. Kivrak, J.R. Havig, T.L. Hamilton, B.L. Teece, Y. He, C. Freissinet, Y. Huang, E. Santos, C. Szopa, A.J. Williams

PII: S0032-0633(24)00117-X

DOI: <https://doi.org/10.1016/j.pss.2024.105953>

Reference: PSS 105953

To appear in: *Planetary and Space Science*

Received Date: 8 March 2024

Revised Date: 26 July 2024

Accepted Date: 8 August 2024

Please cite this article as: Boulesteix, D., Buch, A., Masson, G., Kivrak, L.L., Havig, J.R., Hamilton, T.L., Teece, B.L., He, Y., Freissinet, C., Huang, Y., Santos, E., Szopa, C., Williams, A.J., Environmental Analogs from Yellowstone hot springs on Geochemical and Microbial Diversity with Implications for the Search for Life on Mars, *Planetary and Space Science*, <https://doi.org/10.1016/j.pss.2024.105953>.

This is a PDF file of an article that has undergone enhancements after acceptance, such as the addition of a cover page and metadata, and formatting for readability, but it is not yet the definitive version of record. This version will undergo additional copyediting, typesetting and review before it is published in its final form, but we are providing this version to give early visibility of the article. Please note that, during the production process, errors may be discovered which could affect the content, and all legal disclaimers that apply to the journal pertain.

© 2024 Published by Elsevier Ltd.

# Environmental Analogs from Yellowstone hot springs on Geochemical and Microbial Diversity with Implications for the Search for Life on Mars

D. Boulesteix<sup>1,\*</sup>, A. Buch<sup>1</sup>, G. Masson<sup>1</sup>, L. L. Kivrak<sup>2</sup>, J.R. Havig<sup>3,4</sup>, T.L. Hamilton<sup>3,5</sup>, B. L. Teece<sup>6</sup>, Y. He<sup>7</sup>, C. Freissinet<sup>8</sup>, Y. Huang<sup>9</sup>, E. Santos<sup>9</sup>, C. Szopa<sup>8</sup>, and A. J. Williams<sup>2</sup>,

<sup>1</sup> Laboratoire Génie des Procédés et Matériaux, CentraleSupélec, University Paris-Saclay, 8-10 rue Joliot-Curie, 91190, Gif-sur-Yvette, France

<sup>2</sup> Department of Geological Sciences, University of Florida, Gainesville, FL 32611, USA

<sup>3</sup> Dept. of Plant and Microbial Biology, University of Minnesota, St. Paul, MN, 55108, USA

<sup>4</sup> Dept. of Earth and Environmental Sciences, University of Minnesota, Minneapolis, MN 55455, USA

<sup>5</sup> The BioTechnology Institute, University of Minnesota, St. Paul, MN 55108, USA

<sup>6</sup> NASA Jet Propulsion Laboratory, California Institute of Technology, Pasadena, CA, USA

<sup>7</sup> Institut de Minéralogie, de Physique des Matériaux et de Cosmochimie, Sorbonne Université - CNRS – MNHN, France

<sup>8</sup> LATMOS/IPSL, UVSQ University Paris-Saclay, Sorbonne University, CNRS, 11 Bd d'Alembert, 78280, Guyancourt, France

<sup>9</sup> Department of Geological Sciences, Brown University, 324 Brook Street, Providence, RI 02912, USA.

\* Corresponding co-authors. E-mail address: david.boulesteix@centralesupelec.fr (David Boulesteix)

## Abstract

From Viking landers to Perseverance rover, Mars has been explored by several *in situ* missions capable of analyzing organic compounds. Results from the SAM and SHERLOC on Curiosity and Perseverance, respectively, support the detection of lean organic matter (at ppb-ppm levels) in the top surface samples, although the source(s) and preservation mechanisms are still ambiguous. Perseverance is currently exploring a fluvio-lacustrine system at Jezero crater and may explore an ancient volcanic terrain after exiting the crater. As Perseverance would collect samples for return to Earth, preparation is needed for sample return efforts through various means including i) the detection of trace organic compounds in various matrices, ii) validation of compounds identified by Martian rovers, and iii) better understanding of mechanisms of their production on Mars. On these returned samples, the community may be able to resolve the timing of organic matter formation and refine hypotheses regarding organic preservation in Martian soils despite the presence of numerous oxidants, salts, and pH-temperature intra and inter-site variations that are less conducive to long-term preservation of organic matter. For instance, acidic conditions promote clay catalyzed isomerization, but seem to benefit for the fatty acid preservation producing organic-salts or favoring salt dissolution in the matrix to protect organic compounds from radiations and water alteration. With a similar aim, we selected samples from Yellowstone National Park hot springs and silica sinters as analogs to locations visited by Curiosity and Perseverance or – in the future – Rosalind Franklin rover. The hot springs in this study developed over hundreds to thousands of years, providing optimal conditions (*i.e.*, matrix composition, temperature, pH) of preservation for organic molecules, extremophilic and mesophilic cells. In our study, the most well preserved organic matter and biosignatures were detected in acidic silica sinters with a surface (water) temperature below 50 °C and a minor crystalline phase. The gas chromatography – mass spectrometry molecular analysis revealed a variety of organic compounds we classified as bioindicators (such as amino acids, nucleobases, and sugars), and biosignatures (such as long-chain branched and/or (poly)unsaturated lipids, secondary metabolites involved in the quorum sensing or communication between individuals). We validated with a SAM/MOMA-like benchtop extracting oven the organic matter extraction protocols performed with the SAM experiment. We identified using the different SAM and MOMA extraction protocols (pyrolysis and wet-chemistry derivatizations) eight microbial classes through a unique untargeted environmental metabolomics' method embracing space flight technology constraints. Additionally, we identified one (and likely two) agnostic biosignature(s): i) the concomitance of some elements and organic compounds in the analogs (correlation of organic matter elements: C, N, S, P and organic molecules co-located with essential biological elements: Fe, Mg, V, Mn and non-essential biological elements concentrated by microorganisms: As, Cs, Ga), and ii) the negative isotope C and N ratio demonstrating organic molecules rich in <sup>12</sup>C and <sup>14</sup>N: archaeal, bacterial, and eukaryotic lipids for an efficient low energy-consuming metabolism.

1 **Keywords:** Perseverance rover, Metabolomics, Mars, Hot springs, Terrestrial analogs, Agnostic and  
2 gnostic signatures.

### 3 I. Introduction

#### 4 a. *Exploration of Mars surface and subsurface environments*

5 Mars exploration has leveraged increasingly sophisticated robotics with improving analytical  
6 capabilities, since the first landers (Viking I and II, 1976) and rovers (Mars Exploration Rover, Sojourner,  
7 Mars Pathfinder Mission, 1997), and culminating in the current Curiosity (Mars Science Laboratory  
8 Mission – MSL, 2012) and Perseverance (Mars 2020 Mission, 2021) rovers. The types of flight-ready  
9 analytical capabilities to search for traces of life have expanded from the initial cameras and infrared  
10 (IR) spectrometers in Viking landers-orbiters to a wider range of spectroscopy analyzers. In addition to  
11 infrared and ultraviolet (UV) spectrometers, nowadays, the onboard rovers' analytical suit of  
12 instruments comprise Raman spectrometers analyzing inorganic and organic matter, including the  
13 latest deep ultraviolet laser excitation onboard the Perseverance Raman Scanning Habitable  
14 Environments with Raman and Luminescence for Organics and Chemicals (SHERLOC) instrument [1–  
15 3]. Analytical payloads also carry mass spectrometers to analyze the bulk elemental composition of  
16 organic matter, the isotopic fractionation, and proceed up to the molecular identification [4–6]. The  
17 mass spectrometers have the longest heritage, with the Viking landers [7], followed by the Phoenix  
18 polar lander [8], and the latest landed mass spectrometer in the Sample Analysis at Mars (SAM) from  
19 the MSL mission onboard the Curiosity rover [9].

20 Each mission has explored different formations with potentially preserved organic compounds  
21 for hundreds of millions to billions of years [10] from harsh surface conditions, including drastic  
22 changes in temperature, pressure, and oxidative content of the atmosphere and soils submitted to  
23 energetic solar and galactic radiative particles or photons [11–13]. Since 2012, the Curiosity rover has  
24 explored the 3.5-3.7 Ga Gale Crater, observing hyper-arid and evaporitic clay basins [14–16] rich in  
25 silica (*e.g.*, Opal-A SiO<sub>2</sub>) and different salts/minerals, such as calcium perchlorate (especially in  
26 Yellowknife bay) [17,18], and magnesium sulfate (Mount Sharp) [19,20]. These hyper-arid  
27 environments favor subsurface xero-preservation and protective organo-mineral interactions along  
28 with UV shielding as numerous studies observed on Earth analogs including the Atacama Mars analog  
29 where fossilized cells are well preserved [21–24].

30 Since 2021, the Perseverance rover has explored Jezero Crater, which contains deposits with  
31 Fe/Mg-smectites, other clay minerals, and sediments deposited by water around 3.5-3.6 Ga [25–28].  
32 The depositional history of Jezero was initially interpreted to be a delta [25,26] similar to the  
33 Mississippi delta river in the USA [29]. However, after recent Perseverance investigations, the site may  
34 be better defined as a deltaic fan since the sedimentary deposit characteristics are not specific to being  
35 a delta or an alluvial fan [25]. Near the Octavia E. Butler landing site at Jezero Crater, volcanic activity  
36 from NE Syrtis (on the western edge of Isidis Planitia plain) introduced mafic volcanic units that served  
37 as a source of remnant olivine-bearing carbonate rocks. These deposits and rocks have the potential  
38 to be linked to biotic past traces, such as microbial deposits with concentrated nutrients and light  
39 elements' depletion in sediments or a low erosion rate allowing (bio)signatures xero-pervations in  
40 this unique olivine-bearing unit [26,27] that harbors a wide array of observed mineralogical and  
41 organo-mineral complexes [24,28]. The SHERLOC instrument has been used to identify pyroxene (at  
42 Dourbes), sulfate (at Quartier), and perchlorate (at Guillaumes) salts within the low silica and rich  
43 olivine matrix, as well as predominantly silica samples relatively free from salt (*e.g.*, Alfalfa) [2]. The  
44 carbonate and silica samples collected are thought to be high value targets for detecting traces of life  
45 and diverse organic compounds due to the presence of organo-mineral formations that have a high

1 potential to encapsulate organic materials and protect them from the harsh Mars surface  
2 environment, such as sulfates or sulfur-bearing layers, clays and silica sinters or sediments [21,23,30–  
3 32].

4 The planned Rosalind Franklin rover from the ESA-led ExoMars 2028 mission will explore the  
5 clay-rich Oxia Planum region [33–35]. The rover's payload will include the Mars Organic Molecule  
6 Analyser (MOMA) [36,37], a laser desorption ionization and a gas chromatograph, coupled to a dual-  
7 entry mass spectrometer (GC-MS). One drill will perform a hole up to two meters, and GC-MS analyses,  
8 for the first time, will be done on Mars subsurface samples. In addition to the MOMA instrument, the  
9 Rosalind Franklin rover will embark three other instruments in the Analytical Laboratory Drawer (ALD)  
10 able to detect organic matter, namely the Mars Multispectral Imager for Subsurface Studies (Ma\_MISS)  
11 embedded in the drill tip [153], the MicrOmega [154], and the Raman Laser Spectrometer (RLS)  
12 [38,155]. Results from these future analyses will bring new insight about organic matter preservation  
13 in Martian deep layers that are not impacted by UV and primary X-rays. Secondary X-rays and stronger  
14 energy sources like gamma and cosmic/energetic particles' radiations reach the first few meters, but  
15 with a lower incident energy than within the first centimeters of the Martian regolith. These  
16 destructive processes explain the low detection of organic matter by Viking, Curiosity, and  
17 Perseverance landers/rovers and contribute to the will to drill deeper with Rosalind Franklin rover for  
18 geotopes exposed to low radiation doses at a slower rate [13,39].

19 Following MSL, ExoMars and likely Mars 2020 will investigate volcanically/hydrothermally  
20 driven siliceous sinter precipitates – induced from crater impacts at Gale and Jezero locations.  
21 Scientists discovered these volcanic areas by orbital observations (*e.g.*, at Nili Patera, Arabia Terra,  
22 Oxia Planum) [38,40] that may have preserved organic matter longer than crater locations explored by  
23 MSL (3.6-4.1 Ga). The Curiosity and Perseverance rovers at Gale crater (*Marias Pass*) and Jezero crater  
24 (*Alfalfa*), respectively, analyzed diagenetic silica formations. In the Jezero crater rim and Nili Fossae  
25 region formed from the Isidis Planitia impactor, the heat released by impact may have driven  
26 hydrothermal circulation (*e.g.*, [41,42]). Those input of nutrients and energy millions of years ago  
27 favored proto-cell (and likely evolved life) production following a likely similar pathway to that on  
28 primitive Earth and volcanic/hydrothermal areas. The exploration of those extraterrestrial sites for  
29 past life traces research encompasses the prediction of desired features and the investigation of  
30 conditions and matrices capable of preserving organic matter for millions or even billions of years. To  
31 depict such an environment, elemental and molecular keys are needed to interpret *in situ* and return  
32 sample analysis via mineralogical, elemental-isotopic, and organic matter observations. Such features  
33 might most probably be explained by abiotic/diagenetic processes, thus, we must analyze the  
34 geological context and the bulk elementary and molecular sample to assess organic matter production  
35 mechanisms and potential biogenic character of signatures (as the last resort hypothesis, such as  
36 isotopic biotic fractionation or various compounds with a strong enantiomeric excess).

37 Many Martian silica formations have been attributed to diagenetic processes, according to  
38 orbiter observations and modeling work [43], consistent with observed phyllosilicate content [33,44–  
39 46]. Hydrothermal surface processes (at or below 100 °C) are likely to have occurred billions of years  
40 ago, for instance at Gusev crater, Gale crater, Jezero Crater, and Nili Fossae, or likely Oxia planum.  
41 Volcanic areas may have favor life cell production and organic matter preservation on Mars time scale  
42 [47,48]. Therefore, studying Earth volcanic areas with active hydrothermal deposition of silica and/or  
43 carbonate minerals is of high interest as potential Mars analogs for the following three reasons. First,  
44 to determine the degree of preservation of organic matter in these ancient or modern volcanic  
45 locations; second, to understand the organo-mineral interactions relevant to Mars that might preserve  
46 these potential traces of life (or biosignatures) and third, to estimate the microbial community that  
47 could arise and thrive in these environments to look for precise metabolites (organic compounds used

1 or produced by life) categorized either as bioindicators or biosignatures. Biosignatures can be  
2 compounds, physical structures, isotopic or elemental ratios, and characteristics (*e.g.*, enantiomeric  
3 excess) linked to biotic processes [49] compared to bioindicators that have the same definition with  
4 morphological or composition features explained by abiotic and biotic processes. For instance, Martian  
5 methane production might be due to past life production because it is faster than the photolytic  
6 destruction in Mars atmosphere and in greater quantity than volcanic trapped gas bubbles' release  
7 during successive geological events [50–52]. In addition, if the community finds in the future years  $\delta^{12}\text{C}$   
8 negative value that clearly discriminate biotic from abiotic inputs we could explain the methane  
9 production/preservation with exogenic/atmospheric and surface/subsurface inputs that create  
10 variations in the isotopic  $\delta^{12}\text{C}$  value like clathrate and some matrix that degrades and reduce organic  
11 carbon into methane [53–55].

12 Martian silica rich deposits may benefit from a combination of geophysical characteristics (*i.e.*,  
13 no plate tectonics, slow surface weathering rates, burial by surface regolith, freeze-drying conditions)  
14 with a matrix composition protecting organic matter from physical-chemical alterations (*e.g.*,  
15 radiations, oxidations, erosions) for thousands of years on the surface and million to billions of years  
16 in the subsurface. The preserved organic matter will see a minimal diagenetic degradation in the  
17 subsurface environments where Rosalind Franklin rover will drill [33,56,57]. So far, few organic  
18 compounds have been identified on Mars at Gale Crater, including chlorine-bearing and sulfur-bearing  
19 molecules [30,58–60], present either as such in the sample, or formed from reaction (chlorination,  
20 sulfurization or degradation) occurring in the SAM ovens [61–63]. Organic compounds once altered by  
21 water on Earth or on Mars can either create organo-mineral and organometallic complexes, which  
22 might be the case for Mg/Ca/Fe-perchlorates (co-located with organic matter) on Mars [64–66].  
23 Organic matter is also oxidized and likely aromatized by radiations and/or GC-MS extraction processes  
24 producing PAHs and heteroatom hydrocarbons and aromatics that we observed with SAM and might  
25 be explained in crater systems [30,62,63]. At Gale Crater and other explored locations on Mars, no  
26 bioindicators have been found yet. The current and future exploration of the sulfate-rich Mount Sharp  
27 area by Curiosity, and the sedimentary, and likely the volcanic regions, by Perseverance and ExoMars  
28 will be of high interest to the astrobiology community for many reasons, including the potential to  
29 detect and identify preserved organo-mineral complexes and heavier organic compounds [33].

30 Organic matter fingerprints by gas chromatography (high resolution) mass spectrometry (GC-  
31 (HR)MS) analysis is often used to trace the source of biomolecules and nutrients, including isotopic  
32 analysis on Earth [9,67,68]. Indeed, from the mass spectra of different samples, it is often possible to  
33 identify the biological source of the organic matter, define the distribution pattern of molecules, and  
34 reconstruct metabolic pathways. These metabolites could be preserved in minerals that precipitated  
35 at the time of deposition even if cellular material was not directly preserved, making detection via GC-  
36 MS within the first centimeters of Martian regolith (or meters with the MOMA instrument onboard  
37 ExoMars) possible [36]. Alone these metabolites would not resist to oxidations and radiations, but  
38 within silica or mineral matrix it might be preserved for millions of years [12,13,19,69,70]. The  
39 combination of elemental and molecular analysis will help strengthen the hypothesis on organic  
40 matter preservation conditions and past life traces detection. Thus, we propose in this Mars analog  
41 article to combine different laboratory and space-like analysis to study Yellowstone hot springs as a  
42 Mars analog. Yellowstone samples helped identify signatures/features likely preserved on Mars if  
43 Earth-like life or extent forms of life arose in volcanic/hydrothermal regions. Yellowstone  
44 investigations narrow the most appropriate preservation conditions and environments of organic  
45 matter in extraterrestrial analog geotopes.

46

1  
2  
3  
4  
5  
6  
7  
8  
9  
10  
11  
12  
13  
14  
15  
16  
17  
18  
19  
20  
21  
22  
23  
24  
25  
26  
27  
28  
29  
30  
31  
32  
33  
34  
35  
36  
37  
38  
39  
40  
41  
42  
43  
44  
45

*b. Yellowstone's Mars analog bio-geotopes*

The Sylvan Spring and Geyser Creek Areas (Gibbon Geyser Basin, Yellowstone National Park, Wyoming, USA) are active hydrothermal areas driven by magmatic heating where siliceous sinter precipitation occurs across a range of temperature and pH values. The hydrothermal fluids are influenced by input from the deep magmatic source, dissolution of volcanic bedrock, and interaction with groundwater to produce water saturated with dissolved silica. Hot springs vary in temperature, pH, and geochemical constituents due in part to subsurface processes, including mixing with groundwater/meteoric water and whether near-surface boiling occurs prior to the fluids reaching the surface. Near-surface boiling drives phase separation (vapor phase and residual liquid phase), and the amount of these phases or minimal phase source fluid feeding a hot spring drive the expressed pH and geochemical environment [71]. For example, minimal phase separation hot springs (fed by deep hydrothermal source fluids that have interacted with groundwater to some degree) have similar chloride and sulfate concentrations and have circum-neutral to alkaline pH values (from 7 to 14). In hydrothermal areas where near surface boiling drives phase separation, hot springs that are predominantly vapor phase fed will be extremely low in chloride concentration. Additionally, they will be enriched in sulfide when interacting with O<sub>2</sub> from groundwater or the atmosphere that is readily oxidized to sulfuric acid. This oxidation enriches water in sulfates with pH values of 3 or lower, while a predominantly residual liquid phase hot spring will be enriched in chloride and sulfate (increasing concentration due to boiling). Thus, these liquid phases will have pH values at circum-neutral (with neutral pH being approximate 6.3 at boiling). However, dissolved silica concentrations are high in most worldwide hot spring fluids, with discharging fluids precipitating amorphous silica (*e.g.*, Opal SiO<sub>2</sub>) as silica becomes supersaturated due to decreasing temperatures and/or evaporation [72,73]. Rapid precipitation of silica onto and around endemic microbial communities can effectively preserve textural and geochemical signals generated by life [71,73–76]. However, organic matter can be altered due to overprinting, requiring further study to better constrain the impacts of these effects [75,77].

Temperatures, pHs, and geochemistry parameters impact the composition of the microbial communities present in and around the vent, proximal slopes, distal aprons, and further geothermally influenced environments [71,76,78]. Thus, hot springs can preserve signals from hyperthermophilic to thermophilic chemotrophic communities proximal to vents as well as thermo- to meso-philic phototrophs (*e.g.*, cyanobacteria and other phototrophs [79,80]) and heterotrophs that inhabit environments down the outflow channels (*e.g.*, proximal slope, mid-apron), to low temperature distal aprons where eukaryotic organisms are predominant (*e.g.*, algae, plants, and fungi) [76].

Here, we report results from samples collected from three hot springs in Yellowstone National Park, USA. Silica sinters were sampled to detect and identify textural and organic matter microbial residues to investigate the potential for preservation of biosignatures in hot springs. Particular targets include organic compounds and organo-mineral complexes that might be involved in processes essential for the living microbial community to thrive, and the influence of pH and temperature on the microbial community (and organic matter composition).

The current study has three main objectives: i) the characterization of geobiological and biochemical signatures directly connected to the presence of life in the three Yellowstone hot springs, ii) the identification of micro-niches for organic compound entombment and sheltering, notably by organo-mineral formations, and iii) the identification of the microbial community in the three different geochemical environments according to the environmental pH and temperatures.

## 1 II. Material and Methods

### 2 a. Sample locations

3 Samples were collected from three actively siliceous sinter-precipitating hot springs – Dante’s  
4 Inferno (T 75.9 °C, pH 5.1) in the Sylvan Spring Area, ‘Goldilocks’ (T 45.4 °C, pH 2.4, Yellowstone Thermal  
5 Inventory ID GSSGNN022), and ‘Similar Geyser’ (T 79.3 °C, pH 8.7, Yellowstone Thermal Inventory ID  
6 GGSNN012) in the Geyser Creek Area – located within the Gibbon Geyser Basin, Yellowstone National  
7 Park, USA. Sites represent pH values resulting from different hydrothermal inputs – acidic pH/vapor  
8 phase dominant, mildly acidic to circum-neutral pH/residual liquid phase dominant, and  
9 alkaline/minimal phase separation – with siliceous sinter samples and contextual water samples  
10 collected from zones of active silica precipitation from each site (Table 1).

11 Yellowstone National Park, USA contains a 50 × 80 km diameter 640 Ka volcanic caldera basin  
12 formed from hot-spot volcanic activity relating to a hot lower-mantle plume beneath the North  
13 American Plate, producing dozens of distinct hydrothermal areas with hot springs exhibiting wide array  
14 of temperature, pH, and geochemical characteristics [81]. The Sylvan Springs Area (SSA) in the NW  
15 region of the Gibbon Geyser Basin is an approximately 90,000 m<sup>2</sup> hydrothermal region located on  
16 hydrothermally altered kame deposits overlying glacial till from the ~21 to 13 Ka Pinedale Glaciation,  
17 deposited on Member A of the 640 Ka Lava Creek Tuff [82]. Most of the hot springs occur along a  
18 presumed E-W trending fault cutting through the kame deposit, fed by hydrothermal fluids that have  
19 undergone near-surface boiling and phase separation (with a detailed description of subsurface  
20 processes driving hot spring geochemical expressions in [71]). Hot springs in the SSA can be categorized  
21 as acidic (pH < 3.5) predominantly vapor-phase fed (*e.g.*, ‘Goldilocks’), circum-neutral (pH 5 to 7)  
22 predominantly residual liquid phase (*e.g.*, Dante’s Inferno), or a mixture of these to end members. The  
23 Geyser Creek Area (GCA) in the SE region of the Gibbon Geyser Basin is an approximately 80,000 m<sup>2</sup>  
24 hydrothermal region located on Pinedale glacial rubble and till overlying the intersection of Member  
25 A of the 640 Ka Lava Creek Tuff (NE), the 208 Ka Paintpot Hill Dome of the Mallard Lake Member  
26 Plateau Rhyolite (W), and the 160 Ka Nez Perce Creek Rhyolite Flow of the Central Plateau Member  
27 Rhyolite (SE). Similar to SSA, GCA hot springs are predominantly vapor phase, residual liquid phase, or  
28 a mixture of the two, but there are also limited occurrences of circum-neutral to alkaline (pH > 6.5)  
29 minimal phase separation hot springs (*e.g.*, ‘Similar Geyser’). Siliceous sinter samples were collected  
30 from the active precipitation zone near the photosynthetic fringe in the outflow (46 °C) just below the  
31 primary vent of ‘Goldilocks’ (a digitate structure, GI Dig), from the active precipitation chemotrophic  
32 zone where temperatures had cooled to 25 °C and a nearby abandoned/inactive recent outflow  
33 channel of Dante’s Inferno (DI Active and DI Old, respectively), and from the active precipitation  
34 chemotrophic zone in the outflow channel near the vent (79 °C) of ‘Similar Geyser’ (a digitate structure,  
35 SG Dig).

### 36 b. Sampling procedure

37 Samples were collected with solvent cleaned (methanol and dichloromethane) and heated (at  
38 500 °C for 8 hours in an oven) chisels, spoons, and tweezers. Rock hammers were covered in a piece  
39 of heated (at 500 °C) foil before use then removed for sampling. Samples were placed in these clean  
40 aluminum foil within sterilized glass jars and stored on ice for transport back to the laboratory. Fresh  
41 solvent-washed tools were used for each sample to limit cross-contamination between samples.  
42 Samples were stored at -20 °C freezer in laboratory until analysis. *In situ* analyses have been carried  
43 out to measure temperature and pH of hot spring waters/sinters. Hot spring waters have been  
44 subsamples for isotopic analysis in laboratory.

1 In the laboratory, sinters from glass jars were subsampled by breaking off smaller pieces with  
2 solvent-washed and flamed tweezers. These subsamples were either powdered for 3 minutes with a  
3 ceramic mortar and pestle that have been solvent-washed (methanol, then hexane, then  
4 dichloromethane) and heated (to 500 °C). This grounding step was used to obtain a powdered sample  
5 for X-ray diffraction (XRD), inductively coupled plasma mass spectrometry (ICP-MS), isotopy, total  
6 carbon/organic carbon/inorganic carbon and total nitrogen contents (TC/TOC/TIC and TN), and gas  
7 chromatograph mass spectrometer (GC-MS) analysis. We kept the non-powdered samples for surface  
8 analysis: scanning electron microscope (SEM) and Raman. As samples were carefully collected with  
9 organically clean tools and techniques in the field, samples were not treated to remove potential  
10 natural external contamination before powdering. The MS analyses confirmed the very few (for SG  
11 Dig) or absence of contamination for all powdered samples during the sampling and sample  
12 preparation for the different analyses. Indeed, helium and solvent GC-MS blanks revealed clean  
13 spectra after the analysis of each sample and each replicate with a low background baseline. Moreover,  
14 we did not detect fatty acids or other contaminants from human manipulations (*e.g.*, palmitic acid,  
15 stearic acid, phthalates, etc.) on negative and positive controls we performed on rock powders  
16 simulants without living cells and FAMES' standard to produce the calibration curve.

17 Temperature, pH, and conductivity were measured in situ using a WTW 330i meter and probe  
18 (Xylem Analytics, Weilheim, Germany) and YSI 30 conductivity meter and probe (YSI Inc., Yellow  
19 Springs, OH).

20 Water samples were collected and analyzed as described previously [71]. In short, water was  
21 collected with an acid-washed 140 mL syringe, filtered through a 37 mm, 0.2 µm pore size  
22 polyethersulfone syringe filter, and distributed into cleaned sample bottles for anion, cation, dissolved  
23 inorganic carbon (DIC), and dissolved organic carbon analysis. Samples were kept on ice (anion, cation,  
24 DIC) or frozen (DOC) until analysis. Anion and cation samples were analyzed by the Quantitative Bio-  
25 element Imaging Center (QBIC) at Northwestern University via a Thermo Scientific Dionex ICS 5000+  
26 ion chromatography system and a Thermo iCAP 7600 Inductively Coupled Plasma Optical Emission  
27 Spectroscopy (ICP-OES), respectively. DIC and DOC samples were analyzed by the Stable Isotope  
28 Facility (SIF) at the University of California, Davis via GasBench II system interfaced to a Delta V Plus  
29 isotope ratio mass spectrometer (IR-MS) (Thermo Scientific, Bremen, Germany) for DIC and using an  
30 O.I. Analytical Model 1030 TOC Analyzer (O.I. Analytical, College Station, TX) for DOC.

### 31 c. Imaging and mineralogy of siliceous sinters

32 The samples were gold coated to better resolute the image and be able to conduct energy  
33 dispersive X-ray spectroscopy (EDX) analysis on the four amorphous Opal-A<sub>N</sub> samples. SEM images of  
34 sinter were collected with a Phenom ProX G5 tabletop environmental SEM. Qualitative analyses were  
35 conducted by using a 3 mm spot size, a beam current of 2.25–2.33 nA, and an accelerating voltage of  
36 15 kV under low vacuum conditions consistent with environment SEM operation.

37 Mineralogy was determined on a 0.5-1 g powdered sample through X-ray diffraction with a  
38 PANalytical X-Pert Pro Powder X-Ray Diffractometer (Cu Kα<sub>1</sub> radiation,  $\lambda = 1.540598 \text{ \AA}$ , Emyrean Cu  
39 LFF (9430 033 7300x) at 45 kV and 40 mA) and patterns were acquired from 5° to 70° 2θ (with a 0.0084  
40 ° step size for a continuous scan mode). To semi-quantify we introduced two internal standards that  
41 are not present in the samples with known mineralogical XRD spectrum (*i.e.*, zincite and corundum at  
42 10 wt%) following the methodology of [83]. However, this semi-quantification was not useful since the  
43 abundance in minerals were very low (less than 5 wt% in total) and was primarily composed of quartz.

44 To characterize the organo-mineral structures and correlation spots on the samples and  
45 confirm some XRD mineralogic identification, we first performed Raman analysis on a HORIBA micro-

1 Raman instrument (2-4  $\mu\text{m}$  resolution using a 40x objective, 0.3 D Filter, 200  $\mu\text{m}$  hole) using a 325 nm  
2 ultraviolet (UV) laser excitation source slightly different from the deep-UV (248.6 nm) source onboard  
3 SHERLOC instrument [2]. For the sample preparation, we solvent washed (with ethanol) the plastic  
4 holder to prepare an Epoxy pellet with arising on one of the surface a piece of sample from the broken  
5 pieces (10:1 EpoxySet Resin:EpoxySet Hardener made of bisphenol A and triethylenetetramine,  
6 respectively). The analyzed Raman surface was flattened homogeneously with the fewest frictional  
7 alterations using sequentially 800, 600, 400, 240, 40, and 1  $\mu\text{m}$   $\text{Al}_2\text{O}_3$  sheet (for a final roughness lower  
8 than 1  $\mu\text{m}$ ).

#### 9 d. Elementary analysis of siliceous sinters

10 Elementary analyses were conducted using an Element-2 (Thermo-Finnigan) multi-resolution,  
11 single collector, magnetic sector plasma mass spectrometer (ICP-MS). We used 50 mg of sample that  
12 was digested using first 5:1 eq. vol/vol HF:HNO<sub>3</sub> ultrapure (Optima) solvents for 8h at 100 °C, then by  
13 6N HCl (after HF evaporation) for 8h at 100 °C (evaporated at the end as well). We then added an  
14 aqueous (pure milli-Q grade water (TOC lower than 3 ppb)) solution made of HNO<sub>3</sub> (5%), Re-Rh (8ppb  
15 internal standard), and HF (150 ppm) for 8h at 100 °C. Finally, we used the later solution to dilute by  
16 2,000 the digested mixture. The analyses were made in duplicate and for each analysis, scans were  
17 made in six replicates with a medium resolution of 4,000 and 5 % of error bars in the results.

18 For TIC/TOC/TC/TN and isotopic analyses, we used 20-50 mg of samples to get 20  $\mu\text{g}$  of  
19 nitrogen and 20-200  $\mu\text{g}$  of carbon range. For the organic matter content, we used three standards  
20 called HOS (high organic sediment from Elemental microanalysis), LOS (low organic soil from elemental  
21 microanalysis), and atropine (from Costech analytical technologies). The isotopic analyses were  
22 conducted in six replicates and normalized according to one geological standard close to our siliceous  
23 sinters, namely the HOS standard. It was compared to two organic rich standards usgs 40 and usgs 41  
24 (L-glutamic acids depleted or enriched in <sup>12</sup>C and <sup>14</sup>N, respectively) before and after the samples at two  
25 different concentrations to quantify TC and TN on the wide and unknown content range. TIC analyses  
26 were conducted on a Coulometer CM5017 using a phosphoric acid titration of potential carbonates in  
27 samples. TC, TN, <sup>15</sup>N/<sup>14</sup>N, and <sup>13</sup>C/<sup>12</sup>C analyses were performed by combustion in a Costech Elemental  
28 Analyzer coupled online to a Finnigan-MAT DeltaPlus XL isotope ratio mass spectrometer with a ConFlo  
29 III. For <sup>18</sup>O, we used Ag cups instead of Sn cups (<sup>15</sup>N and <sup>13</sup>C) and a Thermoconvector analyzer. The  
30 values were calibrated to the Vienna Pee Dee Belemnite (VPDB) scale using within-run cellulose  
31 standard Sigma Chemical C6413 calibrated against NBSG DIG9 and NBS22 that were included within  
32 the runs. TOC and TN were measured on the same instrument.

#### 33 e. (Pyrolysis, wet-chemistry, and solid phase micro-extraction)-GC-MS material and 34 preparations of siliceous sinters

35 To perform the organic matter volatilization, we processed the samples using a pyrolysis  
36 method at 600 °C or a wet-chemistry untargeted environmental method with dimethylformamide  
37 dimethyl acetal (DMF-DMA), tetramethylammonium hydroxide (TMAH), or trimethylsulfonium  
38 hydroxide (TMSH). Stainless steel capsules were filled with 5-10 mg sample, 5-10  $\mu\text{L}$  derivatization  
39 reagent (DMF-DMA, TMAH or TMSH), and 1  $\mu\text{L}$  of an internal standard ([D8]naphthalene diluted at 10<sup>-3</sup>  
40 mol L<sup>-1</sup> in dichloromethane – Aldrich, purity > 98% and isotopic purity ~ 99 atom % D). This standard  
41 was chosen because it is inert to the derivatization and thermal processes, and fully vaporized at 500-  
42 600 °C. The capsules were loaded in an EGA/PY-3030D micro-oven pyrolyzer (Frontier Lab). The  
43 pyrolyzer was connected to the Split/SplitLess (SSL) Optic 4 injector (GL Sciences) of a Trace GC Ultra  
44 gas chromatograph coupled to an ISQ LT quadrupole mass spectrometer (Thermo Scientific). The  
45 injector part was set at 300 °C to avoid a cold trap ahead of the GC column. The electronic impact

1 ionization source energy used was 70 eV. The ions produced were analyzed in the m/z range of 40 to  
2 500 u. Analyses were performed in full scan mode.

3 A pyrolysis and derivatization temperature program similar to SAM and MOMA programs were  
4 used with a SAM/MOMA-like extracting pyrolyzer device under Martian conditions for this Mars analog  
5 study. We performed flash pyrolysis and thermochemolysis at 500 °C and 600 °C. To flush organic  
6 compounds into the GC inlet Helium (99,9999% purity, Air Liquide) was used as the carrier gas with a  
7 constant flow rate in the column set to 1.2 mL min<sup>-1</sup>. During the pyrolysis step, the pyrolysates were  
8 trapped with at the chromatographic column head using a cryo-focusing set up cooling down a few  
9 centimeters of the column head to -180 °C. Once the pyrolysis is done, the cooling is stopped and the  
10 column head is quickly heated to the oven temperature. The split flow was 30 mL min<sup>-1</sup>. The MS ion  
11 source was set at 350 °C. The temperature of the transfer line from GC to MS was set to 300 °C.

12 To achieve the separation of the analytes, a 30 m long capillary column (MXT-5, supplied by  
13 Restek) with a 0.25 mm internal diameter and 0.25 mm thick was used. The column was equipped with  
14 a 5 m integrated guard column where the cryotrap was installed to pre-concentrate organics before  
15 GC-MS analysis. The temperature programming of the column started at 50 °C and increased up to 310  
16 °C at a rate of 5 °C min<sup>-1</sup>, and was held for 3 minutes. Blank runs with or without DMF-DMA, TMAH or  
17 TMSH ("solvent-blank" without sample injection) were performed between each sample analysis to  
18 determine and subtract any background level of residual organic matter in the column.

19 The molecular identification with GC-MS was processed by comparison to the National  
20 Institute of Standards and Technology (NIST) reference mass spectra library and using the XCalibur 2.0  
21 software with its peak attribution function. We have been careful to exclude matched molecules with  
22 a Reversed Search Index (RSI) and Similarity Index (SI) lower than 700 – corresponding and inverse  
23 research corresponding factors comparing our mass spectrum of the GC peak selected and the most  
24 similar mass spectrum of the organic molecules from the library. The XCalibur program was also used  
25 to interpret the data.

26 The identification of FAMEs from the analog samples was verified by comparing retention  
27 times and mass spectra of a chromatogram obtained from the analysis of a standard mixture of pure  
28 FAMEs, alkanes, or PAHs (1000 µg mL<sup>-1</sup> each component in hexane – Sigma-Aldrich, 99.9% purity).

29 To quantify the organic recovery and test the reagents' efficiency for each organic molecule,  
30 we measured the peak area of each molecule in the chromatograms and divided it by the peak area of  
31 the internal standard (IS, or [D8]naphthalene) using Thermo Scientific XCalibur software. We also  
32 performed calibration curves with FAMEs, alkanes, and PAHs standards.

$$33 \quad A_{\text{organic}}/A_{\text{internal standard}} = \frac{\text{Area of the organic compound peak}}{\text{Area of the internal standard peak}}.$$

34 On-fiber SPME derivatization headspace extraction was performed loading the derivatizing  
35 reagent on DVB/PDMS SPME fiber by exposing the fiber in a 4 mL vial containing 5 µL of PFBCF or 1 g  
36 of PFBHA at 30 °C or 50 °C, respectively, for 5 min. After that, the loaded fiber was transferred to  
37 another 4 mL vial containing the sample extracted with 0.5 mL of pure milli-Q grade water for 1 h at  
38 30 °C or 50 °C, respectively. 0.5 g of sodium chloride was added to water extraction to improve the  
39 organic compounds volatile.

40 Gas chromatography analysis was performed with an Agilent 6530 GC with, and Agilent 5973  
41 MS operated in electron impact (EI) mode (70 eV) was equipped with a Zebron ZB-1MS gas  
42 chromatography column 30 m x 0.25 mm x 0.25 µm (Phenomenex, USA). The SPME fiber desorption  
43 was operated in the GC inlet at 280 °C in a splitless mode for 5 min using Helium (99,9999% purity, Air

Liquide) as the carrier gas with a constant flow rate in the column set to 1.2 mL min<sup>-1</sup>. The GC temperature was programmed as follows: start temperature of 40 °C (held for 2 min) and increase to 300 °C at 10 °C min<sup>-1</sup> (held for 10 min). The interface GC and MS was set at 310 °C. The temperatures of the ion source and quadrupole were 230 °C and 150 °C, respectively. The mass spectrometer was operated in a mass range of m/z 50 to 500.

### III. Results

#### a. Structural and composition characterizations

##### i. Imaging analysis

First, we characterized geobiological and biochemical signatures to look for the preservation of organic matter and cells in the three hot springs from acidic to basic pH [2.39; 8.72] range.

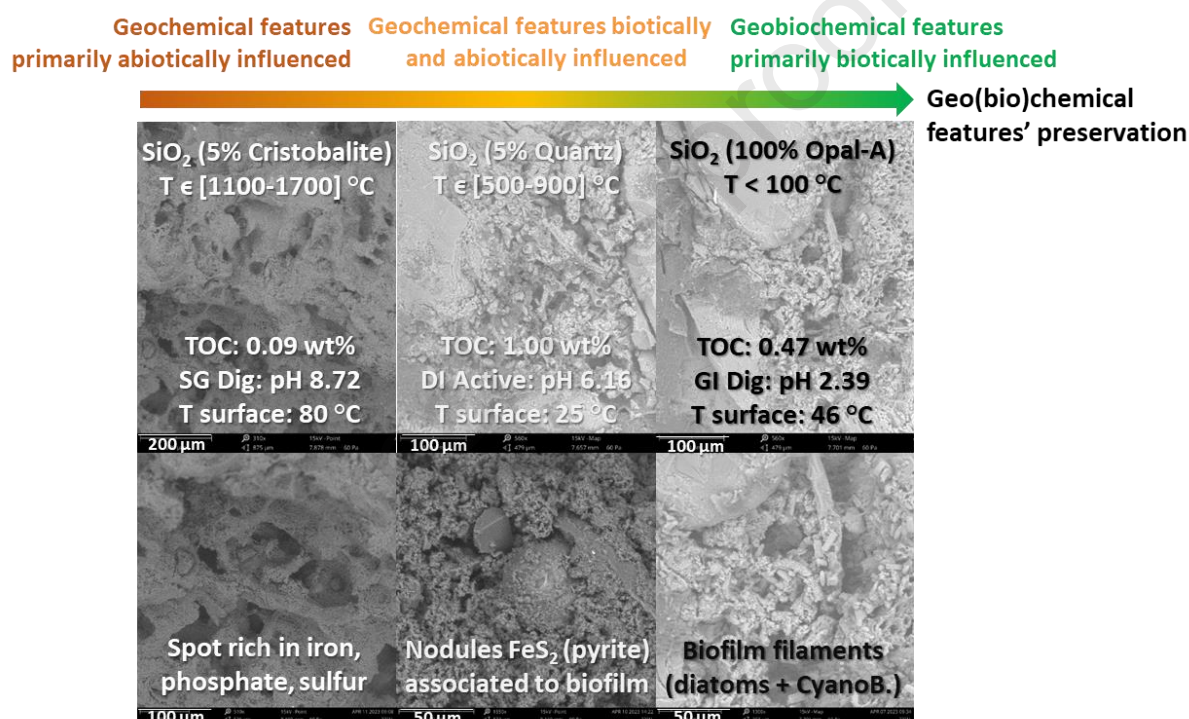


**Fig. 1.** Physical and elementary results based on SEM-EDX, temperature and pH probes, TOC, and XRD analysis following a pH gradient that might follow a biotic-abiotic geo(bio)chemical feature preservation gradient in samples collected in poly-extreme (SG Dig) to mesophilic (DI Active) environments.

SEM-EDX imaging (Fig. 1 and Supplementary Material 1 – SM1) was used to characterize the sample surface, internal structure, and primary elemental composition. First, we visually observed green pigmented biofilms on the surface of GI Dig and confirmed by SEM visualization of biofilm filaments (Fig. 1 and SM1). We also noted yellow chemotrophic biofilms on the sample at the time of collection due to different pH biotopes. Second, the EDX analysis helped confirm the presence of (bio)geological features, such as pyrite nodules observed as well in previous studies in the same springs (Dante's Inferno and 'Goldilocks') [84] or filaments (in 'Goldilocks samples') (SM1). We noted in SEM-EDX imaging the enrichment in iron and sulfur, or in nitrogen, carbon, and phosphorous, to the nodule and biofilm formations, respectively. We noted the preservation of morphological cell signatures in the most acidic samples along with a broader diversity and content range in heteroatoms.

## ii. Elementary analysis

**Table 1.** Physical-chemical characteristics of siliceous sinters and associated hydrothermal water.

	'Goldilocks'	Dante's Inferno		'Similar Geyser'
	GI Dig	DI Active	DI Old	SG Dig
<b>Water pH</b>	2.39	6.16	6.16 (estimated)	8.72
<b>Water temperature (°C)</b>	45.70	25.10	25.10 (estimated)	~80
<b>wt% C (= TOC)</b>	0.47	1.00	0.26	0.09
<b>wt% N</b>	0.07	0.07	0.05	0.02
<b><math>\delta^{13}\text{C}</math> (‰, vs. VPDB)</b>	-17.21	-23.78	-21.03	-11.50
<b><math>\delta^{15}\text{N}</math> (‰, vs. Air)</b>	-2.31	-3.68	1.09	6.42
<b><math>\delta^{18}\text{O}</math> (‰, vs. VSMOW)</b>	5.55	10.45	8.33	-1.63
<b><math>\delta^{18}\text{O}</math> (‰, vs. VSMOW) of surface water samples</b>	-14.33 ‰	-9.34 ‰	N.D.	-14.79 ‰
<b>Rhyolite quartz <math>\delta^{18}\text{O}</math> [85,86]</b>	4.3 ‰	7.6 ‰	7.6 ‰	N.D.
<b><math>^{51}\text{V}</math> (MR)</b>	0.0004%	0.0008%	0.0004%	0.0004%
<b><math>^{33}\text{Cs}</math> (MR)</b>	0.0001%	0.0030%	0.0030%	0.0383%
<b><math>^{31}\text{P}</math> (MR)</b>	0.0049%	0.0059%	0.0030%	0.0039%
<b><math>^{75}\text{As}</math> (MR)</b>	0.0065%	0.0060%	0.0055%	0.0052%
<b><math>^{24}\text{Mg}</math> (HR)</b>	0.0000%	0.0180%	0.0010%	0.0117%
<b><math>^{39}\text{K}</math> (HR)</b>	0.1679%	1.2882%	0.1460%	0.2487%
<b><math>^{44}\text{Ca}</math> (HR)</b>	0.2566%	0.3383%	0.2370%	0.3434%
<b><math>^{56}\text{Fe}</math> (HR)</b>	0.1816%	0.5790%	0.1730%	0.6686%
<b><math>^{69}\text{Ga}</math> (MR)</b>	0.0002%	0.0018%	0.0003%	0.0160%
<b><math>^{55}\text{Mn}</math> (HR)</b>	0.0040%	0.0064%	0.0053%	0.0053%
<b><math>^{23}\text{Na}</math> (HR)</b>	0.2680%	0.7826%	0.3320%	0.8601%
<b><math>^{27}\text{Al}</math> (HR)</b>	0.3903%	2.5590%	0.3410%	0.6620%
<b><math>^{32}\text{S}</math> (TQ and CHNOS)</b>	1.1750%	7.2727%	0.8667%	0.4500%

N.D.: no data, HR: high resolution, MR: medium resolution from the ICP-MS analyzer. Sulfur was detected thanks to a CHNOS and ICP-MS triple quadrupole analyzers.

We conducted ICP-MS elemental analysis to quantify what we observed in SEM-EDX analysis to confirm hypothesis on the Fe-S amount present locally or uniformly in the matrix, for instance. A low concentration in iron and sulfur would lead as first approach to biotic concentration around the biofilm and biological filaments observed in SEM-EDX. On the opposite, an overall high concentration would most likely lead to an input from the surrounding water that precipitated within collected silica sinters and would remain available for the hypothetical populations observed in SEM-EDX (Table 1 and SM1).

The most abundant elements in the amorphous silica samples, except silicon and oxygen are iron, sulfur, sodium, and aluminum, then calcium and potassium. These results confirm the high abundance of Fe (and S with a triple quadrupole ICP-MS) precipitates observed in SEM-EDX. The

1 quantity of  $\sim 0.1-0.6\%$  on average and for some specific sulfur-rich locations between  $1-7\%$  (SM1)  
 2 might reveal organisms' species based on sulfur metabolisms (*e.g.*, organisms in DI Active and GI Dig).  
 3 Previous studies on other alkaline hot springs have reported the enrichment of Mn, Fe, Ga, and S  
 4 associated with preserved microbial traces or cells as we also report for SG Dig (SM1) [71,74].

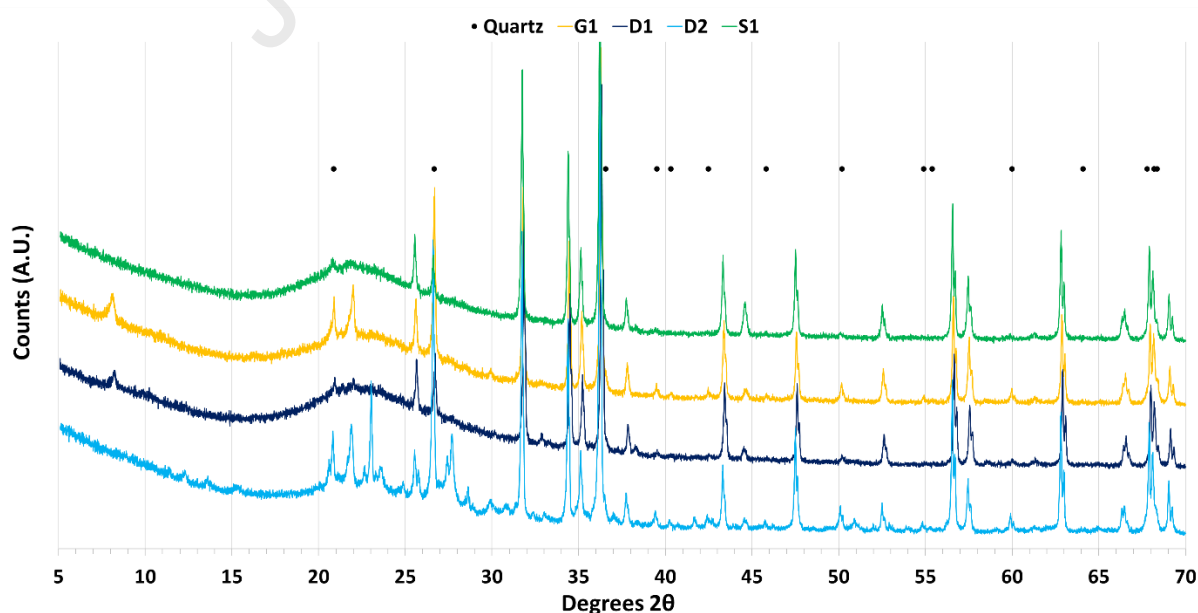
### 5 *iii.* Isotopic analysis

6 In Table 1, we reported the isotopic measurements of three main elements: i) carbon from  
 7 organic matter to identify enrichment in  $^{12}\text{C}$  due to microbial autotrophic ( $\text{CO}_2$ -fixing) metabolisms  
 8 [87]; ii) nitrogen in organic matter to identify potential  $^{15}\text{N}$  depletions or enrichments indicative of  
 9 microbial mediated nitrogen redox reactions; and iii)  $^{18}\text{O}$  to track geophysical signature to retrace the  
 10 geological history of the site and the sample.  $^{18}\text{O}$  tracks the temperature variations in the geological  
 11 layers, and finally  $\delta^{18}\text{O}$  demonstrates the depletion in  $^{16}\text{O}$  by oxygenic species due to some  
 12 photosynthetic organisms (*e.g.*, algae).

13 The most negative  $\delta^{13}\text{C}$  and  $\delta^{15}\text{N}$  values were observed in samples with the lowest surface  
 14 water temperature, as observed in previous studies with the same  $\delta^{13}\text{C}$  values [88] meaning the most  
 15 abundant microbial community in cooler spring pools, discriminate  $^{13}\text{C}$  from  $^{12}\text{C}$  for their metabolism.  
 16 This result is consistent with the reduced number of organisms that can tolerate temperatures higher  
 17 than  $65\text{ }^\circ\text{C}$  (thermophilic and hyperthermophilic extremophiles).

### 18 *iv.* Minerals connected to organic matter and their likely interaction

19 The overall mineralogy determined by XRD analyses of the four samples were made of an  
 20 amorphous opal- $\text{A}_\text{N}$  silica phase that contain 1 to 5 % of crystalline phase in addition to the 0.1 to 1 %  
 21 of organic carbon observed with TOC analyses (Table 1 and Fig. 2). The crystalline phase includes quartz  
 22 (present in all samples), cristobalite ('Goldilocks'), and pyrite (Dante's Inferno). The relatively older  
 23 precipitates collected from compacted areas not directly in the outflow of Dante's Inferno (DI Old)  
 24 contained higher percentage of quartz compared to modern precipitates from this active hot spring,  
 25 interpreted as early diagenesis that already occurred compared to fresh silica precipitates at the  
 26 surface of the hot spring (DI Active). However, no pyrite was detected most likely due to the low wt%  
 27 in the samples.



28

1 **Fig. 2.** XRD spectra of the four samples with the two internal standards (zincite and corundum) and the  
2 most abundant crystalline form observed (quartz).

3 The Raman spectroscopy with a UV laser excitation source helped confirm the major minerals  
4 and the co-localization of some minerals (*e.g.*, pyrite) with organic matter (SM2). We first noted the  
5 difference between the Raman spectrum of the epoxy polymeric matrix without organic matter  
6 detected and the locations where the samples arisen with trapped organic matter before interpreting  
7 organo-mineral correlations (SM2).

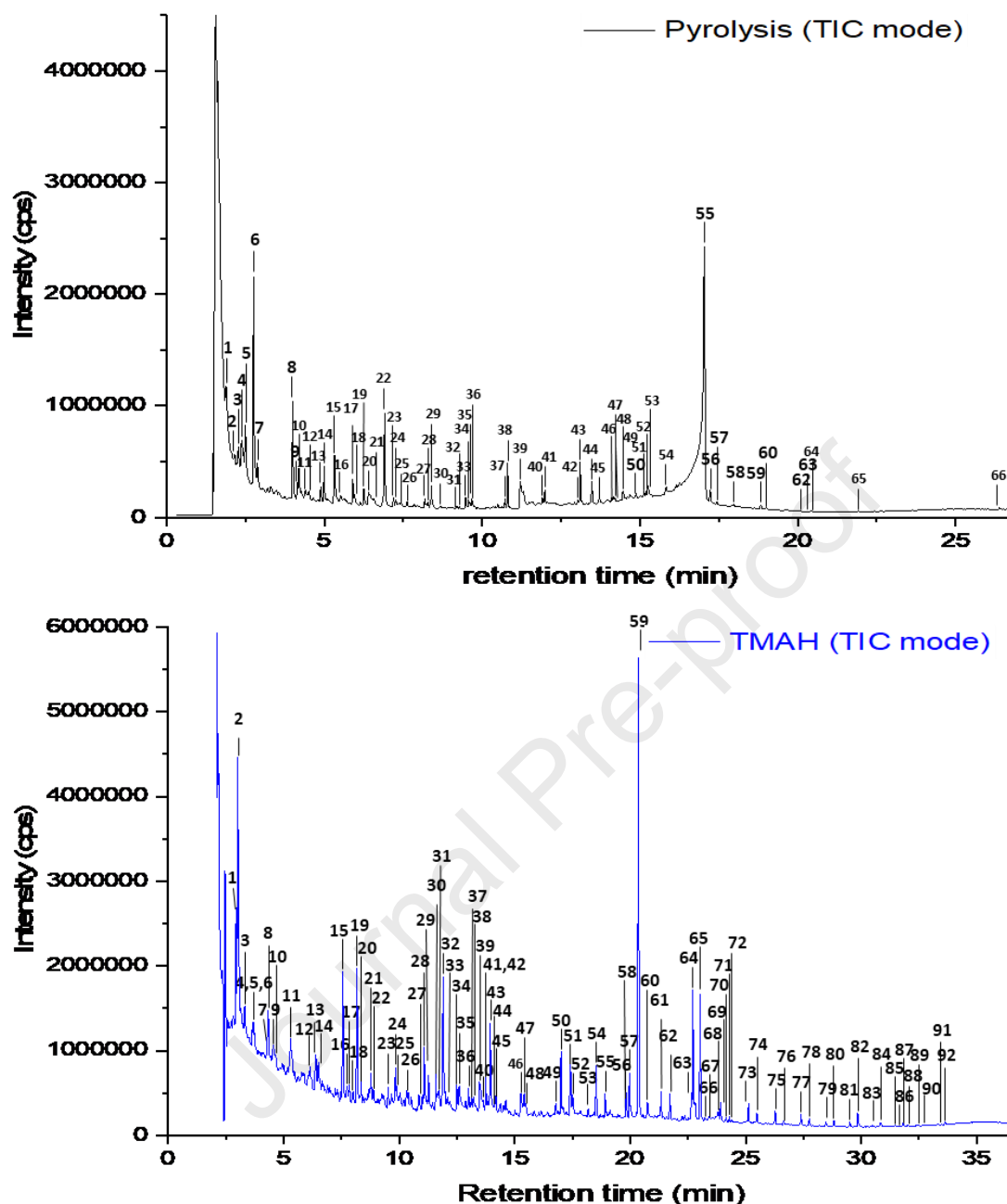
8 In the Raman analysis (SM2), we observed organic matter likely associated with the  
9 degradation of lipids and other metabolites – with the Raman D and G bands due to defect in graphitic  
10 structure and C-C bond from  $sp^2$  orbital, respectively, but also a weak band of C-O-C at  $800\text{ cm}^{-1}$ , a  
11 weak band characteristic of carboxylic acid dimer at  $910\text{--}960\text{ cm}^{-1}$ , and likely aromatic rings between  
12  $990\text{--}1050\text{ cm}^{-1}$ ,  $1365\text{--}1450\text{ cm}^{-1}$ ,  $1450\text{--}1505\text{ cm}^{-1}$  within the carboxylic acid, D and G bands. Indeed,  
13 they are associated rather than originated from the environment since we observed in GC-MS analyses  
14 a low abundance of (a)biotic native PAHs produced in hydrothermal process in low proportion  
15 comparing hot spring apron and further precipitates. Specifically, we observed the G-band  
16 characteristic of kerogens ( $1500\text{--}1600\text{ cm}^{-1}$ ) (SM2). For the samples with and without epoxy (SM2), we  
17 observed few peaks at  $450\text{--}490\text{ cm}^{-1}$ ,  $550\text{--}600\text{ cm}^{-1}$ , and  $700\text{--}850\text{ cm}^{-1}$ , consistent with the  
18 predominantly silica matrix and previous works on similar matrix and environments [2,89].

#### 19 a. Lipidic and metabolomic analysis

20 Following elemental analysis, we conducted molecular analysis to interpret the microbial  
21 community diversity, the organic matter preservation in different environmental conditions, and the  
22 efficiency of SAM and MOMA sample processing and analysis to extract and detect biosignatures.

23 As explained in the material and methods, the MS analyses confirmed the very few (for SG Dig  
24 less than 10 % of the analytes' quantity) or absence of contamination for all samples during the  
25 sampling and sample preparation for the different analyses. Thus, we did not need to prepare the  
26 sample by solvent-wash or sterilization at  $50\text{ }^\circ\text{C}$  for few hours in order to free from human  
27 contaminations to get less than 10 % in quantity, especially in palmitic and stearic acids.

28



1  
2 **Fig. 3.** Total Ion Chromatograms of TMAH and pyrolysis pre-treatments on GI Dig (modern “Goldilocks” – Sylvan  
3 spring siliceous sinter) where we identified the following organics (different from the solvent by-products) with  
4 few dozens more compounds observed selecting 43, 57, and 143 u)

5 **For Pyrolysis:** 1: Butanal, 3-methyl-; 2: (N-(2-acetamido))-2-aminoethanesulfonic acid; 3: 1H-pyrrole; 4: Toluene;  
6 5: Pyrrolidine, 2-butyl-1-methyl, 6: Furfuraldehyde; 7: 1H-pyrrole, 1-methyl-; 8: 2-furancarboxaldehyde, 5-  
7 methyl; 9: Phenol, 10: 1H-pyrrole-2,5-dione; 11: 2,2-dimethyl-4-octenal; 12: 1H-pyrrole-2-carboxaldehyde; 13:  
8 Thiophenone; 14: Benzeneacetaldehyde; 15: Phenol, 3-methyl; 16: Undecanol; 17: Levoglucosenone; 18:  
9 Succinimide; 19: Benzene, 1-isocyano-2-methyl-; 20: D8-naphthalene (internal standard); 21: Unknown  
10 compound; 22: Benzofuran, 2,3-dihydro-; 23: Glucopyranose, 1-thio-, 1-(N-hydroxybenzenepropanimidate); 24:  
11 Tridecene; 25: Tridecane; 26: Indolizine; 27: o-tolunitrile, a-cyano-; 28: Benzene, heptyl-; 29: Bicyclopentyl-2,2'-  
12 dicarboxaldehyde; 30: Hexadecanol; 31: nonadecane; 32: 1H-indole, 1-methyl-; 33: Carbonimidodithioic acid,  
13 methyl-, dimethyl ester; 34: Octadecenal; 35: Heptadecane; Hexathiane; 36: Cetene; 37: Hexadecane; 38:  
14 Eicosene; 39: Nonadecene; 40: Phenol, 3-phenoxy; 41: Thiosulfuric acid, S-(2-(cyclopropylamino)-2-iminoethyl)  
15 ester; 42: Hexacosene; 43: Sulfurous acid, hexyl octyl ester; 44: Cyclic octatomic sulfur; 45 to 47: Unknown  
16 compounds; 48: Tetracosane; 49: Hexadecanenitrile; 50: Unknown compound; 51: Dipentamethylenethiuram

1 hexasulfide; 52: 2-pentadecylfuran; 53: Unknown compound; 54: Tetratetracontane; 55 to 59: Unknown  
 2 compound; 60: Carbonic acid, eicosyl vinyl ester; 61 to 66: Unknown compound. The peak 55 that has a  
 3 significant peak area belongs to a sulfur-bearing compound.

4 **For TMAH:** 1: 4-aminopyridine ; 2: Methanesulfonic acid, methyl ester; 3: 2,4-dithiapentane; 4: Unknown  
 5 compound; 5: Dimethyl sulfone; 6: Ethyl methyl sulphone; 7: 2-furancarboxaldehyde, 5-methyl; 8: 1,2,4-  
 6 trioxolane, 3-phenyl-; 9: Glyceraldehyde, dimethyl ester; 10: Benzene, (methoxymethyl)-; 11: Butanedioic,  
 7 dimethyl ester; 12: Phenol, 3-methyl; 13: 2,5-pyrrolidinedione, 1-methyl-; 14: Benzoic acid, methyl ester; 15: D8-  
 8 naphthalene (internal standard); 16: Hepta-2,4-dienoic acid, methyl ester; 17: 1,3-benzenediol, 4-ethyl-; 18 to  
 9 22: Unknown compounds; 23: Benzaldehyde, 4-methoxy-; 24: 1H-indole, 1-methyl-; 25: Carbonimidodithioic  
 10 acid, methyl-, dimethyl ester or 1,3-dithiole-2-thione; 26: Unknown compound; 27: Heptadecane; 28: 1,3-  
 11 dimethyl-3,4,5,6-tetrahydro-2(1H)-pyrimidinone; 29: Phenol, 3,4-dimethoxy-; 30: Proline, 1-methyl-5-oxo-,  
 12 methyl ester; 31: 1,2,4-trimethoxybenzene; 32: Unknown compound; 33: 2,3,6-triO-O-methyl-Galactopyranose.  
 13 34: Unknown compound; 35: 2,3,4-trimethyllevoglucosan; 36 and 37: Unknown compounds; 38: Nonadecene;  
 14 39: 2,4(1H,3H)-pyrimidinedione, 1,3,5-trimethyl-; 40: Unknown compound; 41: 2,4,5,6,7-  
 15 pentamethoxyheptanoic acid, methyl ester; 42 and 43: Unknown compounds; 44: Pentadecane; 45: Unknown  
 16 compound; 46: Hexacosene; 47: Dodecanoic acid, methyl ester; 48: Tetracosane; 49: Unknown compound; 50:  
 17 Hexadecane; 51: Diethyl phthalate; 52: 2-propenoic acid, 3-(4-methoxyphenyl)-, methyl ester; 53: Methyl  
 18 tetradecanoate; 54: 9H-purin-6-amine, N,N,9-trimethyl-; 55: Tetratetracontane; 56: Unknown compound; 57:  
 19 Octadecane; 58: Pentadecanoic acid, methyl ester; 59: Pentadecanoic acid, 14-methyl, methyl ester; 60: GlcA-  
 20 DG, permethylated; 61: Hexadecanoic acid, methyl ester; 62: 5,10-diethoxy-2,3,7,8-tetrahydro-1H,6H-  
 21 dipyrrolo[1,2-a:1',2'-d]pyrazine; 63: Eicosane; 64: Heptadecanoic acid, methyl ester; 65: Heneicosane; 66: 9-  
 22 octadecenoic acid, methyl ester; 67: Stearic acid, methyl ester; 68: Fluoranthene; 69: Methyl 10,15-  
 23 dimethoxycarbonylhexadecanoate; 70: Methyl 9-cis, 11-trans-octadecadienoate; 71: Docosane; 72:  
 24 Cyclopropanoic acid, 2-octyl-, methyl ester; 73: Nonadecanoic acid, methyl ester; 74: 2,4,6(1H,3H,5H)-  
 25 pyrimidinetrione, 1,5-diethyl-3-methyl-5-phenyl-; 75: Pentacosane; 76: Eicosanoic acid, methyl ester; 77: Methyl  
 26 14-methyl-eicosanoate; 78: Octacosane; 79: Methyl 20-methyl-heneicosanoate; 80: Nonacosane; 81: Tricosanoic  
 27 acid, methyl ester; 82: Heptacosane; 83: Tetracosanoic acid, methyl ester; 84: Unknown compound; 85: Methyl  
 28 17-methyl-tetracosanoate; 86: Unknown compound; 87: Hexacosanoic acid, methyl ester; 88 to 91: Unknown  
 29 compounds; 92: Octacosanoic acid, methyl ester.

30 In flash pyrolysis, we observed on all three sites numerous products from the hot spring  
 31 community, especially in alkene (C<sub>1</sub>-C<sub>20</sub>) and heteroatom compounds compared to the wet-chemistry  
 32 treatments. We observed less alkanes in pyrolysis compared to the TMAH and TMSH analyses on all  
 33 samples with a ratio of even and odd alkanes above two and above a hundred in quantity (checked  
 34 based on the retention time of a pure alkanes' standard) of C<sub>13</sub>-C<sub>25</sub> in pyrolysis and C<sub>13</sub>-C<sub>44</sub> using wet-  
 35 chemistry. We remarked very few lipids detected by pyrolysis compared to wet-chemistry process.  
 36 Derivatization process extracted lipids and related acids from C<sub>1</sub> to C<sub>18</sub>. Goldilocks sample, however,  
 37 ranged up to C<sub>28</sub> that might be explained by acidic pH waters where heavier n-fatty acids like  
 38 octacosanoic acid (boiling point at 430.5 °C) are produced in higher quantity for their acidophilic lipid  
 39 membrane. On the opposite, we detected benzene, toluene, and fluoranthene for Goldilocks' sample  
 40 and all pre-treatments. Together with the lipid analysis by TMAH and TMSH, we can reconstruct a part  
 41 of the microbial community and identify the following families/orders for each sample (Table 2).  
 42 Overall, the fatty acid-lipidic profile in Fig. 3 and Table 2 is explained by two main communities. The  
 43 first community demonstrating the major shorter straight and (poly)unsaturated n-alkanes' and n-fatty  
 44 acids' chain (< C<sub>20</sub>) with an even number of carbon atoms (with in addition the cyanobacterial C<sub>17</sub>) are  
 45 associated to eukaryotic and bacterial microbial inputs, whereas longer chains with an odd number of  
 46 carbons are allocated to higher plants located in the coast of hot-springs only [90,91].

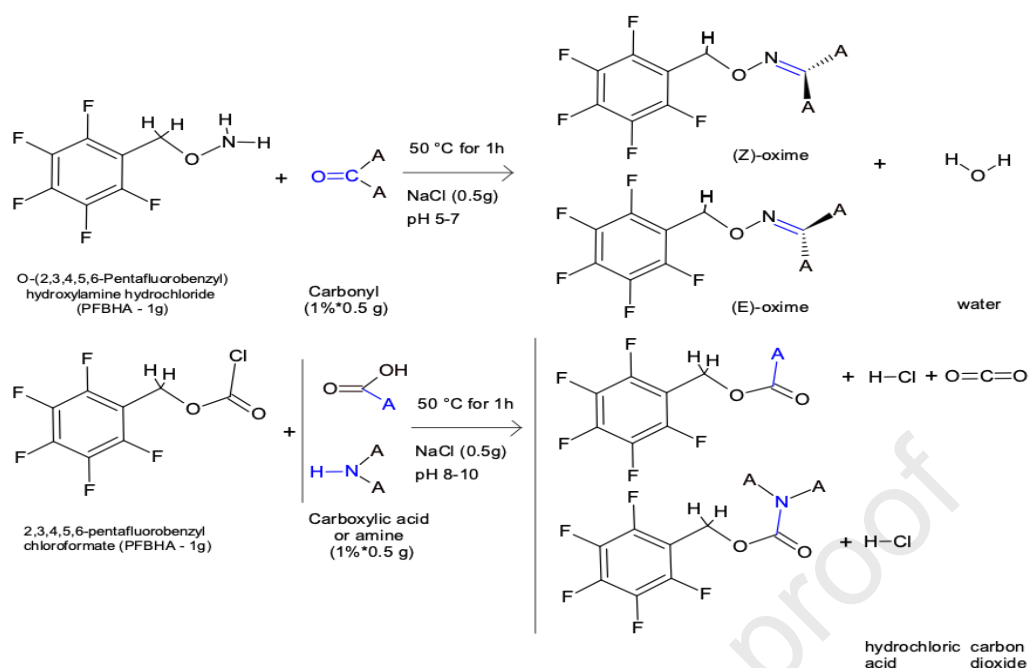
**Table 2.** Selection of interesting gnostic biosignatures (and bioindicators for the light organic compounds below  $C_{12-16}$ ) or their derivatives (due to biological or chemical transformations) cross-link with literature and the huge effort furnished in previous studies in Yellowstone hot spring systems. These biomolecules might be interesting target to look for during future Mars analysis specific to certain class of metabolites in function of the endemic or extremophilic populations towards the different GC-MS pre-treatments.

Class of metabolites	Actinomycetes [92]	Algae [93]	Cyanobacteria [94,95]	Metabionta	Thermoacidophiles archaea and acidophilic/thermophilic bacteria [96–99]	Euglenophyta [100]	Alkaliphile archaea [96,97]	Sulfate-reducing bacteria [101]	GC-MS pre-treatment
Linear/saturated fatty acid (FA)	From palmitic acid to arachidic acid ( $C_{16}$ - $C_{20}$ )	From palmitic acid to melissic acid ( $C_{16}$ - $C_{30}$ )	From palmitic acid to arachidic acid ( $C_6$ - $C_{24}$ )	From palmitic acid to melissic acid ( $C_{16}$ - $C_{30}$ )	From palmitic acid to melissic acid ( $C_{16}$ - $C_{30}$ )	From palmitic acid to arachidic acid ( $C_{16}$ - $C_{18}$ )	From palmitic acid to arachidic acid ( $C_{16}$ - $C_{20}$ )	From palmitic acid to arachidic acid ( $C_{18}$ - $C_{20}$ ) higher abundance than $C_{16}$ - $C_{17}$ )	TMAH TMSH DMF-DMA
Mono-unsaturated fatty acid (MUFA)	N.D.	From 6-heptenoic acid to 11-eicosenoic acid ( $C_7$ - $C_{20}$ )	From 9-tetradecenoic acid to 9-octadecenoic acid ( $C_{14}$ - $C_{18}$ )	From 9-tetradecenoic acid to 9-octadecenoic acid ( $C_{14}$ - $C_{18}$ )	Vaccenic acid ( $18:1\omega-7$ ) from bacterial lipids	Palmitoleic acid and oleic acid ( $16:1$ and $18:1\omega-9$ )	N.D.	Vaccenic acid and oleic acid ( $18:1\omega-7$ , $18:1\omega-9$ )	TMAH TMSH
Poly-unsaturated fatty acid PUFA	N.D.	8,11-octadecadienoic acid and $\alpha$ -linolenic acid ( $C_{18}$ from fresh water algae)	9,12-octadecadienoic acid ( $18:2$ ) and $\alpha$ -linolenic acid ( $18:3\omega-3$ )	9,12-octadecadienoic acid ( $18:2$ ) and $\alpha$ -linolenic acid ( $18:3\omega-3$ )	9,12-octadecadienoic acid that might be from archaeal lipids	$\alpha$ -linolenic acid ( $18:3\omega-3$ )	N.D.	N.D.	TMAH TMSH
Archaeol	/	/	/	/	Glycerol and tridecanoic acid, 4,8,12-trimethyl-	/	Glycerol and tridecanoic acid, 4,8,12-	/	TMSH

					(that might come from for instance diphytanyl glycerol) from archaeal lipids		trimethyl- (that might come from for instance diphytanyl glycerol)		
Glycerol dialkyl glycerol tetraether (GDGT)	Glycerol	/	Glycerol, galactose that might come from MGDGs and DGDGs.	/	Glycerol, isoprenol, isopentol, mevalonate	Glycerol, galactose that might come from MGDGs and DGDGs.	Glycerol, isoprenol, isopentol, mevalonate	Glycerol, isoprenol, isopentol, mevalonate (only gram-positive metabolites detected)	TMAH TMSH
Diether	/	/	/	/	Octanoic acid, methoxy-, 8-dodecenoic acid, methoxy-, hexadecanoic acid, methoxy-	/	Octanoic acid, methoxy-, 8-dodecenoic acid, methoxy-, hexadecanoic acid, methoxy-	Octanoic acid, methoxy-, 8-dodecenoic acid, methoxy-, hexadecanoic acid, methoxy-	TMAH TMSH
Hopanoid	N.D.	N.D.	N.D.	N.D.	N.D.	N.D.	N.D.	N.D.	/
Alkanol	N.D.	1-dodecanol, 3,7,11-trimethyl-	N.D.	1-dodecanol, 3,7,11-trimethyl-	N.D.	1-dodecanol, 3,7,11-trimethyl-	D.D.	N.D.	TMAH TMSH
Sterol and poly aromatic hydrocarbon (PAH)	cyclopentanoph énantrénique	Furan, 2-heptyl, p-cresol, 1H-indole, isoquinoline	N.D.	Furan, 2-heptyl, p-cresol, 1H-indole, isoquinoline	cyclopentanoph énantrénique	N.D.	cyclopentanoph énantrénique	cyclopentanoph énantrénique	Pyrolysis TMAH TMSH
Glycolipid	Galactoseptanoside, Glucopyranoside, and decycled: (e.g., 2,4,5,6,7-pentamethoxyhe	Galactoseptanoside, glycerol	N.D.	Galactoseptanoside, glycerol	N.D.	Galactoseptanoside, glycerol	N.D.	N.D.	TMAH TMSH

	ptanoic acid) with linear lipids identified.								
Peptidoglycan	Glucosamine and few amino acids (e.g., norvaline)	/	Glucosamine and few amino acids (e.g., norvaline)	Glucosamine and few amino acids (e.g., norvaline)	N.D.	Glucosamine and few amino acids (e.g., norvaline)	N.D.	N.D.	TMAH TMSH
Other lipidic compounds (and derivatives)	Mycolic acids (e.g., Octanoic acid, 8-hydroxy-, carynomycolic acid)	Betaine that might be connected to the saturated FA, cinnamic acid, terephthalic acid	/	Betaine that might be connected to the saturated FA, cinnamic acid, terephthalic acid	16-methylhexadecanoic acid, 15,16-dimethyltriacontandioic acid from bacterial lipids and Benzenepropanoic acid, 4-methoxy	/	N.D. (phospholipids)	8-methylnonanoic acid, 16-methylhexadecanoic acid, 15,16-dimethyltriacontandioic acid	TMAH TMSH
Sugar and derivative	Glucose, glycerol	Glucose, glycerol	Glucose, glycerol	Glucose, glycerol	N.D.	Glucose, glycerol	N.D.	Glucose, glycerol	TMAH TMSH

N.D. : Not detected (other than compounds put in other box from the same class of organisms).

1 *iii. Solid phase micro-extraction GC-MS analysis*

2  
3 **Fig. 4.** SPME PFBHA and PFBCF reactions and GC-MS analysis results with the list of compounds  
4 identified and specified for the one derivatized.

5 **Table 3.** List of volatile organic compounds detected after evaporation at 50 °C for 1h on the fiber  
6 where PFBHA or PFBCF derivatization could occur to be observed in GC-MS.

Compound name	PFBHA	PFBCF
Toluene	X	X
Pentanal, 3-methyl-		X
Formaldehyde*	X	X
Hydroxylamine*	X	X
Acetaldehyde*	X	X
Hexanoic acid, 2-ethyl-		X
Acetone*	X	X
Benzoic acid		X
Carbonic acid*		X
2-sec-butylcyclohexanone		X
Propionaldehyde*	X	
Octanoic acid	X	
Isobutanal*	X	
Butyraldehyde*	X	
Nonanoic acid	X	X

1,3-dihydropropanone*		X
Butanal, 2-methyl*	X	
Pentanal*	X	
2,4,4-trimethyl-3-(3-methylbutyl)cyclohex-2-enone	X	
Unknown compound	X	X
Decanoic acid	X	X
Acetic acid*		X
3-methylpentanal*	X	
Hexanal*	X	
2,5-cyclohexadiene-1,4-dione, 2,6-bis(1,1-dimethylethyl)-	X	
Heptanal*	X	
Dodecanoic acid	X	
Diethyl phthalate	X	
7,9-di-tert-butyl-1-oxaspiro(4,5)deca-6,9-diene-2,8-dione		X
Octanal*	X	
Benzaldehyde*	X	
Crotonaldehyde*	X	
Phenylacetaldehyde*	X	
Nonanal*	X	
Hexathiane	X	
Phtalic acid	X	
Glycoldial*	X	
Diglycolic acid*	X	X
Decanal*	X	
1,2-benzenedicarboxylic acid, bis(2-methylpropyl) ester	X	
Ethanone, 2,2-dimethoxy-1,2-diphenyl	X	
7,9-di-tert-butyl-1-oxaspiro(4,5)deca-6,9-diene-2,8-dione	X	
Unknown compound	X	
Unknown compound	X	
Dibutyl phthalate	X	X
Hexadecanoic acid	X	
2-methyl-2-pentenal*	X	

Cyclic octaatomic sulfur	x	
Glutaraldehyde*	x	
Benzyl butyl phthalate	x	x

\* derivatized compounds by PFBHA/PFBCF

1 We identified numerous compounds using the SPME fiber method (Table 3 and Fig. 4) that  
 2 revealed complementary identifications to pyrolysis and thermochemolysis GC-MS analyses, especially  
 3 with the detection of light aldehydes, amines, ketones, carboxylic acids, and PAHs. For the latter, we  
 4 identified toluene that might be a by-product of pigment lipids by diagenetic reactions. Indeed, organic  
 5 matter alteration after disassociation of lipids from cell membranes by bio-chemical processes  
 6 including hydrolysis, redox, (de)sulfurization, for instance on polyene isoprenoids [78]. This hypothesis  
 7 might be strengthening with the other pigment by-products identified. Regarding aldehydes and  
 8 ketones, the origin might be from fermentation and oxidant-reduction energetic thermophilic  
 9 processes [102,103]. These compounds identified on modern, but also on ancient silica sinters  
 10 demonstrate the hypothesis that cells entombed by silica precipitation help preserve physical  
 11 structure and cellular organic matter [104] on Earth and extrapolated to other planetary systems like  
 12 Mars. Therefore, based on the overall lipidomics (and metabolomics) work, we identified several  
 13 bioindicators and primarily gnostic biosignatures within the geobiological, geochemical, and  
 14 biochemical studies (Table 2).

#### 15 IV. Discussion

16 The study was focused on Yellowstone National Park hot springs' systems analog to past active  
 17 volcanic areas or induced hydrothermal systems in Martian crater regions with the aim to depict and  
 18 differentiate abiotic to biotic then agnostic to gnostic signatures of past or present life. The samples  
 19 from Dante's Inferno and 'Similar Geyser' were collected from chemotrophic zones of their respective  
 20 outflows with numerous nutrients bioavailable within a neutral or basic pH (*e.g.*, phosphate, arsenate,  
 21 and sulfate). Indeed, organisms are drawing their energy from mineral substrates with a renewable  
 22 source of S, P, Fe, K, Na, Mg, Ca, V, Mn, Co, Ni, Cu, Zn, Mo thanks to the active hot spring outflows.  
 23 However, in SEM-EDX, we did not observe sheltered living/fossilized cells or C, N, and P traces from  
 24 the desiccated biomass for GI Dig and very few for DI Active and DI Old compared to SG Dig. The  
 25 observation of pyrite nodules led to the hypothesis that they were globules of elemental sulfur trapped  
 26 in silica and subsequently consumed by organisms in acidic environment with pyrite precipitation  
 27 replacement [84]. The correlation between imaging and spectroscopic analysis helped constrain the  
 28 influence of pH and temperature on the potential preservation of siliceous sinters. Based on these  
 29 surface analyses, pH seemed to be the main driver of the present microbial community diversity and  
 30 the resultant silica that precipitated. However, temperature was most likely the primary driver for  
 31 organic matter and microbial abundance in these systems similarly to other hot springs' systems. In  
 32 addition, from SEM analysis, we noticed that silica precipitates at several millimeter scales for alkaline  
 33 pH or at the free ion state at acidic pH with nodules or other crystalline or amorphous phase at 100  $\mu$ m  
 34 to few mm scale related to water temperatures. In all samples, the EDX analyzer detected carbon- and  
 35 sulfur-rich patches where organic matter was correlated to the presence of traces of life observed in  
 36 SEM (filaments, globules, EPS matrix in SM1). These results provide a valuable input on the preserved  
 37 active microbial community being currently in the early diagenesis process of these hot springs [75].

38 Some geological features (*e.g.*, pyrite nodules, silica precipitate preserving biological textures)  
 39 may represent bioindicators – forming as a result of active or passive biological processes – and not  
 40 biosignatures due to potential abiotic processes that might produce features with similar shape and  
 41 composition, making their detection in Martian samples ambiguous. However, isotopic analyses

1 (coupled to molecular mass spectrometry techniques) may provide stronger determination of  
2 biological provenance because living organisms fractionate elements in favor of their lighter isotopes  
3 to save energy during the transport and the metabolization of nutrients. Isotopic fractionation thus  
4 represents an agnostic bioindicator or biosignature since only living organisms produce strong  
5 fractionations in favor of light elements [114–117]. These signatures might also be important for  
6 prebiotic chemistry because they are the locations of potential autocatalytic and organic chemistry  
7 reactions that might lead to primitive cells [118]. Other signatures clearly indicate biogenicity, such as  
8 preserved cellular structures/textures and enrichment of co-located C, N, S, and P (Fig. 1 and SM1).  
9 While on Earth, these first order discriminations are often based on visual and elementary analyses,  
10 current spaceflight missions are not equipped with the capability to image and analyze on micro- to  
11 nano-meter scales. Therefore, we must correlate these observations with complementary  
12 spectroscopic and mass spectrometry analysis to classify spectral signatures as organic molecules or  
13 nutrients essential to life, bioindicators, or biosignatures. This classification would help demonstrating  
14 the biogenicity of an analog or extraterrestrial sample. SEM-EDX analyses revealed physical evidence  
15 of microbial processes with the oxidation of elemental sulfur spheres coated with extracellular  
16 polymeric substances (EPS) biofilms. The biomass clearly noted as filaments and confirmed by a rich  
17 organic content in localized EDX and Raman analysis with smaller spheres irregularly shaped due to  
18 localized oxidations. The microbial community in acidic environments mediated Fe-S mineral  
19 precipitation (and confirmed with GC-MS analyses the presence of pyrite and/or organic matter),  
20 consistent with previous work [84].

21 Several chemical elements were detected in high abundance for all samples relative to Fe and  
22 S (*i.e.*, Na, Ca, K, Mg especially for DI Active) and additional elements co-localized to organic matter  
23 (*i.e.*, P, Cs, As especially in SG Dig), according to SEM-EDX and Raman analysis. For Na, Ca, K, Mg, Mn,  
24 and V, we hypothesize the presence of minerals in low abundance within the silica matrix (below 5  
25 wt%), *i.e.*, halite, vanalite, corvusite, fritzscheite, rollandite, and hyalophane. Some of them were  
26 observed in previous works in Yellowstone hot springs and likely correlated to microbial communities  
27 [71]. The microbial life assimilates elements for their metabolism (*i.e.*, Mg, V, Mn, Fe, Co, Ni, Cu, Zn,  
28 Mo) and releases organic compounds (compatible osmolites and EPS matrix) to agglomerate soil  
29 particles and minerals (non-essential biological elements, *i.e.*, Si, Li, Al, Ga, As) to protect themselves  
30 from environmental stress [119,120]. These hypotheses have been confirmed by analyzing  
31 surrounding rhyolites enriched in the same elements without biofilms in previous studies and other  
32 hot spring locations [71,84,88]. These elements might be helpful to produce organo-mineral  
33 complexes and thus help precipitate organic matter on the surface [121]. This phenomenon is essential  
34 for organic matter and cell preservation over a long geologic time scale in these volcanic systems on  
35 Earth and likely Mars. Indeed, the study of organo-mineral complexes might provide a clue to discover  
36 (geobiological or biochemical) biosignatures or bioindicators if we first detect a patch of sulfates or  
37 pyrite, for instance, and second if we detect organic matter co-located with these minerals on Mars.

38 However, the presence of sulfates and pyrite has never clearly given an answer to the  
39 preservation of organic matter over million to billions of years even if it remains a strong hypothesis  
40 based on carbon-sulfur chemistry [30]. Thus, geospatial chemical analysis, such as a Raman mapping  
41 of organic matter and minerals on a sample might help localize organo-minerals complexes and  
42 biosignatures on Mars. In this study, the Raman mapping (SM2) co-located quartz, opal A, and organic  
43 matter. However, we did not quantify several % of pyrite or other minerals that may help preserve  
44 organic matter, except silica. The bulk analysis in XRD or the surface analysis of Raman did not succeed  
45 to identify with certainty pyrite, however, small nodules and fractions of Fe-S minerals have been  
46 detected in SEM-EDX in located places of DI Active and GI Dig. This lack of detection is explained by

1 the low wt% of these minerals in the samples and the local precipitation at the negligible 10-50  
2 micrometer scale compared to the centrimetric scale of the sample, or the few millimeters resolution  
3 in Raman. The amorphous silica, and in minor ways the Fe-S crystalline forms producing phyllosilicate  
4 sheets and spherical capsules, respectively, helped preserve relatively small amounts (0.1 to 0.26 wt%  
5 of the least preservation site SG Dig and most ancient site DI Old) of organic matter and cells in active  
6 Yellowstone hot springs.

7 Concerning the elements associated with organic matter in our samples, we detected  
8 phosphorus, which is essential for the energetic metabolism of all microbial life on Earth, and we also  
9 detected relatively high concentrations of As and Cs. These metals are associated with organic matter  
10 in geothermal systems and contaminated soils due to mining or industrial factories [119,120]. As and  
11 Cs are metabolized by some extremophile organisms [120,122–125]. The high percentage in Cs,  
12 especially in alkaline silica sinters (SG Dig), is relevant for our research because on Earth, as on Mars,  
13 Cs is generally present in soils at around a few ppb to ppm [121], except when concentrated by a  
14 volcanic event and/or by life (associated to organic matter as remarked in SEM-EDX). The relationship  
15 between As and life is explained by biotic processes that use these metals for oxidative-reductant  
16 reactions for electron exchange in the energetic or secondary metabolisms. The concentrations of As  
17 did not show a particular trend in its enrichment relative to pH compared to Cs. Arsenic behaves like  
18 phosphorus as oxy-anions, however, As is toxic for microbial life, as opposed to P, which is essential  
19 for energetic metabolisms. Microorganisms adapted to As-rich environments can either reduce and  
20 precipitate the cation or methylate arsenate anions that volatilize [123]. In the three YNP hot-springs  
21 investigated here, the amount of As ranged in the same order of magnitude than P, demonstrating  
22 that As is reduced and precipitates as a cation, rather than being methylated, because As would have  
23 been volatilized and escaped from the silica sinters [71].

24 If on Mars, or other planetary systems, we observe i) a few percentages of these two elements  
25 co-located with organic matter and ii) note the detection of As precipitates due to pH that is influenced  
26 by life and in a minor way by geological events, which are rare on Mars compared to Earth in volcanic  
27 areas, we might hypothesize that life may have arisen on the explored site. This primitive life might  
28 have used Cs and P for their metabolisms while they precipitated As in order to access P (or  $\text{PO}_4^{3-}$ ). The  
29 validation of those hypotheses on Mars might be easier if we find a correlation between organic matter  
30 and As/Cs concentrations, or if As and Cs are concentrated in restrictive volcanic areas compared to  
31 surrounding volcanic soils. This correlation would work as bioindicator, and links with other elements  
32 like the high concentration of pyrite or high molecular weight organic compounds (above  $\text{C}_{16}$ ), for  
33 instance, would lead to a biosignature.

34 The exploration for hot spring deposits in volcanic systems or from large impact craters on  
35 Mars should be a critical analysis and sampling goal for rover missions due to past traces of sustainable  
36 water and energy for organic matter to react. The current study and the will to detect these inorganic  
37 and organic markers suggest that the instrumentation on board current and future rovers should be  
38 ideally suited for detection of geochemical and textural evidence of life (*i.e.*, detection of the  
39 biologically important elements C, N, P as well as trace elements such as Mn, Co, and Ni ; identification  
40 of relevant mineralogy such as amorphous silica, opal, iron-sulfides, and arsenic ; and quantitative  
41 identification of organic matter).

42 Finally, elementary analysis revealed macroscopically and then microscopically photosynthetic  
43 populations on the shelf further from the hot waters, which correlate with the depletion in  $^{16}\text{O}$  (SG  
44 Dig). Compared to other hot spring fluids, the investigated biotopes were enriched in  $^{16}\text{O}$  (DI Active  
45 and Old), which means these samples had a lower biomass than silica sinters. The enrichment in  $^{16}\text{O}$  in

1 the acidic silica sinters (GI Dig, DI Active, DI Old) compared to alkaline sinter (SG Dig) is explained by  
2 the tradeoff between: i) the fractionation (depletion in  $^{16}\text{O}$ ) in the fluvial precipitation for low surface  
3 temperature in silica sinters; ii) the enrichment in  $^{16}\text{O}$  from rhyolite signals and may be contributed to  
4 the sinters by input from ground volcanic rocks; and iii) in a minor role due to an active microbial life  
5 in acidic hot springs. Indeed, despite the modern silica sinters collected, we noted a difference with a  
6  $^{16}\text{O}$  enrichment in silica sinters compared to surrounding waters used to precipitate silica (Table 1).  
7 Thus, we might hypothesize that microbial life plays a role in the release of oxygen in the precipitation  
8 with an input of  $^{16}\text{O}$ , balancing the depletion of  $^{16}\text{O}$  from spring waters [87], which might lead to  
9 another bioindicator marker. Microbial life cannot produce some essential metabolites like some  
10 amino acids or sugars, therefore, they need to absorb it from the soil and water to operate their  
11 metabolism. This metabolic processes favor the integration of lighter C,N,O-bearing compounds and  
12 lighter elements within these inorganic and organic cells' compounds.

13 The only agnostic biosignature in our analysis is represented by a negative isotopic value for  
14 carbon. The lowest  $\delta^{13}\text{C}$  value at  $-23.78\text{‰}$  (compared to  $-11.50\text{‰}$ ) likely reveals the activity of the  
15 photosynthetic biofilms in DI Active (and GI Dig) coolest hot springs. The (hyper)thermophiles do not  
16 use the reductive pentose phosphate cycle (PEP) to fix carbon but the reductive tricarboxylic acid cycle  
17 (TCA) that fractionates  $^{13}\text{C}$  differently: from  $-5$  to  $-10\text{‰}$  for TCA cycle and  $-17$  to  $-27.5\text{‰}$  for PEP cycle.  
18 However, these specific values cannot be by themselves biosignatures for a specific classes of  
19 organisms (phototrophs with PEP cycle and chemotrophic with TCA cycle) because some chemotrophic  
20 organisms use instead of TCA the acetyl coenzyme A pathway (ACP) where the  $^{13}\text{C}$  fractionation range  
21 from  $-5$  to  $-28\text{‰}$  [88,126]. Despite the overlap of  $\delta^{13}\text{C}$  values, a negative value in  $\delta^{13}\text{C}$  remains an  
22 agnostic biosignature because no geological-physical-chemical abiotic process allows such a  
23 fractionation in  $\delta^{13}\text{C}$ .

24  $\delta^{15}\text{N}$  values in DI Active and GI Dig are close to zero, which corresponds to the isotopic  
25 composition of the atmospheric  $\text{N}_2$ , demonstrating a strong input of nitrogen from aeolian deposition  
26 (and inorganic solutes like nitrates). Therefore, nitrogen is the limiting factor in silica sinters' biofilms  
27 with limited concentrations in nitrogen found in SEM-EDX and elementary TN analyses without  
28 detection of nitrate in the mineralogical and elementary analyses. This limiting nitrogen is mostly  
29 observed in SG Dig with a strong positive value [88,127].

30 The TOC analysis,  $\delta^{13}\text{C}$  values, and  $\delta^{15}\text{N}$  values together would strengthen the discovery of past  
31 traces of life or prebiotic chemistry on the Early-Mars surface, if they present a strong depletion in  
32 heavy elements with a high concentration in TOC, as we observed in the modern Dante's Inferno site.  
33 Indeed, if we compare DI Active with the older layers DI Old collected at Dante's Inferno or SG Dig (at  
34 Similar Geyser) the higher temperatures favor different communities with different metabolisms that  
35 is presented in this untargeted environmental metabolomics study. Temperatures above  $50\text{--}70\text{ °C}$   
36 decrease the preservation of organic compounds especially in alkaline soils (with or without a high  
37 abundance of oxidants, *e.g.*, perchlorates, sulfates).

38 In the literature, scientists revealed that biosignatures would most probably be preserved in  
39 alkaline and temperatures below  $70\text{ °C}$  [58,75,76,128,129]. These conclusions based on temperature  
40 are consistent with the present study where the least organic matter preservation is in the hottest hot  
41 spring (above  $70\text{ °C}$  all year long). However, the highest organic content and microbial life biosignatures  
42 and bioindicators preservation were within the acidic hot springs (*i.e.*, GI Dig and DI Active sinters).  
43 Therefore, temperature seems to pressure the most organic matter preservation. pH seems to drive  
44 in a minor way microbial life and organic preservation in volcanic and hydrothermal systems, but still  
45 significantly with an order of magnitude between acidic and circum-neutral or alkaline hot springs.  
46 Concerning geobiological signatures, the acidic pH seems to favor organic compounds' and/or cells'  
47 preservation at YNP on the opposite of non-volcanic areas where alkaline environments seem to favor  
48 the preservation in silica sinters [128]. Alkaline environments preserve biosignatures longer than acidic

1 ones in different Earth environments due to the co-precipitation of organic matter and cells with  
2 minerals and salts. The latter may protect organic matter from oxidation, erosion, and radiations.  
3 However, in hot springs and volcanic geotopes, if the temperature is above 50-70 °C, the co-  
4 precipitation might be either too slow before organic matter degradation or does not allow the long-  
5 term preservation with a constant water alteration at high temperatures (above 70 °C). Therefore,  
6 alkaline geotopes seems to be the best location to investigate on Mars, especially for silica precipitates,  
7 clays, or sediments, except for volcanic/hydrothermal-driven environments where the acidic and  
8 sulfur rich regions would be most hopeful for organic matter and biosignatures detection on the first  
9 radiated and oxidized centimeters or meters, according to Yellowstone and Mars SHERLOC and SAM  
10 analysis.

11 Raman analyses demonstrated that UV laser source help detect organic compounds if well  
12 preserved. SHERLOC instrument uses deep-UV laser source, compared to the UV laser source used in  
13 this work, which allows for a finer detection of organic matter at the microscale. The sampling process,  
14 Raman analysis methodology, and laser sources used on Yellowstone and Mars samples helped detect  
15 from 10-100 ppm to % of organic matter. However, none of the results highlight clearly the presence  
16 of biosignatures. Laboratory Raman revealed the presence of bioindicators (likely connected to gnostic  
17 biosignatures) and confirmed by GC-MS. Indeed, together with SEM-EDX and ICP-MS, we may suggest  
18 the presence of life in the sample with concomitance of organic matter elements (C, N, S, and P) with  
19 metabolized elements (Mg, V, Mn, Fe) and non-essential biological elements pre-concentrated by  
20 organisms (Al, Ga, As, Cs) due to biotic concentration processes. Therefore, we need complementary  
21 analysis to confirm the hypothesis of co-precipitation between organics and minerals or mineralization  
22 of elements induced by certain classes of organisms through a molecular analysis (GC-MS) to depict  
23 the metabolites used and track back the classes of organisms that are present (in support of previous  
24 genomic analysis).

25 To ensure the microbial signal detection in a natural sample and quantify biosignatures that  
26 were associated and/or protected within the siliceous sinter samples, we conducted lipidomic and  
27 untargeted environmental metabolomics analyses. We compared these data with previous studies  
28 investigating Yellowstone hot springs and microbial community composition by DNA/RNA sequencing.  
29 Previous analyses of samples from Dante's Inferno via 16S rRNA-sequencing confirmed a rich  
30 chemolithotroph community based on sulfur and iron metabolisms [71]. The authors of that study also  
31 assumed that the  $S^0$ -oxidizing bacteria may be associated with generation of EPS matrix with a dense  
32 biofilm entombed and fossilized in these sulfur spheres during the oxidation process. Members of the  
33 microbial community were associated with iron ( $Fe^{III}$ ) reducing bacteria and archaea including  
34 *Hydrogenothermales*, *Desulfurococcales*, *Thermoproteales*. In addition to chemolithotroph  
35 populations, photoautotrophs are present in the 'Goldilocks' outflow (where the water temperature  
36 is below 72 °C and sulfide concentrations do not inhibit phototrophy), including cyanobacteria and  
37 algae [80]. These photosynthetic organisms produce an abundant amount of organic matter for their  
38 metabolic input, leading to higher concentrations of TOC in the modern precipitate samples compared  
39 to other sites (*e.g.*, DI Old) or hot springs with a lower biomass (*e.g.*, SG Dig chemotrophic zone).

40 The detection in GC-MS (pyrolysis mode) of alkene ( $C_1$ - $C_{20}$ ) and heteroatom compounds  
41 compared to the wet-chemistry treatments revealed, for most of them, the origin of these organics.  
42 Indeed, these compounds are metabolite by-products degraded at 600 °C during pyrolysis rather than  
43 originated from the sample since in SPME-GC-MS and wet-chemistry processes, we did not observe  
44 these numerous unsaturated products and few alkanes. These later few alkanes, however, observed  
45 with derivatization processes demonstrated their production by certain microbial populations in these  
46 extreme environments, see Tables 2 and 4.

1 On Mars with SAM experiments, we successfully detected alkanes up to C<sub>12</sub> and carboxylic acid  
2 up to C<sub>9</sub> (and likely C<sub>12</sub>), in addition to benzene and naphthalene [30,62,63,67,130,131]. In this analog  
3 study with hydrothermal vents that might mimic induced hydrothermal systems in the Gale crater  
4 investigated by MSL, we observed these low molecular weight organic compounds with, for most of  
5 them, a correlation with current life metabolisms. However, as a single molecule or without heavier  
6 organic compounds, we cannot extrapolate the detection of these gnostic biosignatures with potential  
7 past life on Mars since no strict biosignatures were noted in MSL analysis. First, because these  
8 compounds are produced abiotically as observed in meteoritic and returned asteroid samples [132–  
9 135]. Second, on Mars, we did not detect heavy molecular weight compounds like peptidic or nucleic  
10 polymers or agnostic biosignatures [30,59], such as a negative isotopic fractionation for carbon or  
11 nitrogen or co-localization of molecular biosignatures with nutrients or toxic elements trapped in a  
12 biofilm matrix by organisms to feed or protect from their environment. The study of the first  
13 centimeters on Mars might be biased by the harsh oxidative and radiative environment that destroy  
14 evidence of potential past life traces [1,13,136].

15 Carboxylic acids of abiotic and fatty acids of biotic origin produce distinctly different profiles in  
16 GC-MS analyses, since, based on carboxylic acid abundance, the peak demonstrating the most  
17 abundant carbon-chain size in the Gaussian curve of acids distribution differ. The peak is around C<sub>16</sub>-  
18 C<sub>18</sub> for biotic origins (as noted in this study and previous works [137–139]) while the carbon ranges  
19 from C<sub>1</sub> – C<sub>30-32</sub> thanks to enzymatic elongations. On the opposite, abiotic processes do not reveal a  
20 carbon preference within the overall range from C<sub>1</sub> – C<sub>8-12</sub> [132,133]. Moreover, we noticed a specific  
21 biosignature related to the shape of the main fatty acids detected, which were long straight chains of  
22 even carbon greater than the odd one due to enzymatically formed acetyl units (C<sub>2</sub>) derived from  
23 glucose by the major species of Yellowstone hot-springs [78,84,140].

24 The lipidic analyses remain the most powerful tool in metabolomics studies to get a sense of  
25 the broad community diversity. Pyrolysis analyses helped first observe aromatics, alkanes, and alkenes  
26 that correlate with Raman observations. Indeed, the Raman bands were primarily due to lipids  
27 degradation. Second, TMAH and TMSH revealed the identification of 28 esters and three ethers  
28 present in GI Dig related to eukaryotic and bacterial populations. In contrast, the SG Dig exhibited a  
29 greater number of ethers and a distinct variety of esters, particularly those with heavy molecular  
30 weight fatty acids ranging from C<sub>16</sub> to C<sub>30</sub>. These compounds enable resistance to high temperatures,  
31 a characteristic typically associated with archaeal and hyperthermophilic bacteria classes (Table 2). On  
32 the opposite, in DI Active and Old, we noticed the light molecular weight straight chain fatty acids and  
33 two to three orders of magnitude higher in C<sub>16</sub> and C<sub>18</sub> (higher enrichment by 2-10 compared to the  
34 other samples) due to the phototrophic populations [137] observed on the field and in SEM. In Dante's  
35 Inferno samples, C<sub>16</sub> and C<sub>18</sub> fatty acids (that are methylated by TMAH/TMSH to be detectable by GC-  
36 MS) were the most abundant in modern, compared to ancient precipitates. Indeed, a more diverse  
37 and abundant community was detected on the few samples analyzed in the modern towards the older  
38 samples demonstrating the quantity of C<sub>16</sub> and C<sub>18</sub> an order of magnitude higher in DI Active. Same  
39 conclusions for the increase in alkanes and PAHs in DI Old due to the degradation of microbial life and  
40 organic matter over hundreds to a thousand years by hydrothermal, erosion, temperature, and likely  
41 pH (according to SEM-EDX and Raman analysis coupled to GC-MS) parameters.

42 The untargeted environmental TMAH method allowed the detection and relative  
43 quantification of numerous sulfur-bearing compounds that are thio-metabolites – useful in the  
44 energetic and/or communication metabolisms of thermo/acidophilic extremophiles in SG Dig and GI  
45 Dig. The pyrite minerals are revealed by products formed in the pyrolyzer at 500 °C (*e.g.*, cyclic  
46 octaatomic sulfur). In addition, we detected few amines, alcohols, and aldehydes useful in the  
47 thermophilic-resistant metabolism, such as phenols (*e.g.*, phenol, 3-methyl- or phenol, 2-methoxy-)

1 that promotes electron transfer and are key to driving the humification of organic substances [141],  
2 2,3,6-trio-O-methyl-galactopyranose involved in the energetic metabolism. We observed several  
3 primary metabolites produced by most of the organisms on Earth (*e.g.*, glyceraldehyde, 1H-indole-  
4 methyl, 1-methyl-5-oxo-proline), and few by-products of these microbial metabolites (*e.g.*, different  
5 alkanes (C<sub>16</sub>-C<sub>44</sub>), alkenes (C<sub>2</sub>-C<sub>6</sub>), aromatics and PAHs (C<sub>6</sub>-C<sub>16</sub>)).

6 Therefore, the organic diversity revealed a part of the hot springs' community with about 50-  
7 150 compounds detected in each sample (Tables 2 and 4). 20-25% of these organic compounds are  
8 lipid-derivatives and 20-30% are by-products of lipids and other primary metabolites. Indeed,  
9 hydrothermal fluids alter, by oxidation and decarboxylation reactions the lipids, for instance, depicting  
10 a similar quantity of lipids and alkanes or aromatics. Some of these detected alkanes and aromatics  
11 are not only by-products of pyrolysis process or hydrothermal alterations, but also represent a  
12 secondary metabolites used to communicate between individuals, to feed or find nutrients, and/or to  
13 protect themselves like monomethyl alkanes in cyanobacteria. In addition, we noted the presence of  
14 several 1,2-di-O-alkylglycerols (diethers) and hopanoids characteristics of bacterial and archaeal  
15 metabolism and membranes [142,143]. As observed in previous studies, we also noticed that  
16 temperature (more than pH) tends to influence the length of hydrocarbon-chain for thermostability of  
17 the lipidic membrane above 40 °C, such as C<sub>16</sub>-C<sub>20</sub> to C<sub>20</sub>-C<sub>30</sub> straight fatty acids for hyperthermophiles  
18 or bacterial and archaeal diethers [137,144,145].

19 We detected the dominant archaeal lipids that include archaeol and glycerol dialkyl glycerol  
20 tetraethers (GDGTs) in high temperature hot springs towards thermophilic species (SG Dig, GI Dig, and  
21 in fewer quantity in DI Active to resist to acidic pH that might slightly vary seasonally even if the  
22 temperature does not vary) [113-116]. In GI Dig, we discovered a lots of by-products coming from the  
23 mevalonate (MVA) pathway rather than the 2-C-methyl-D-erythritol 4-phosphate (MEB) pathway for  
24 the biosynthesis of isoprenoids. This observation leads to the hypothesis that the most acidic hot  
25 spring favors diversity in archaea and acidophilic bacteria lineage rather than in eukaryotic and gram-  
26 negative bacterial lineage [96,97,146]. The detection of some isoprenoids, mevalonate, and branched  
27 or multi-unsaturated alkenes (especially from three to five saturations are certain metabolites) due  
28 to decarboxylated fatty acids or terpenoids and isoprenoids degradation. These compounds could be  
29 a biosignature in Martian samples if they are detected along with their by-product derivatives. The  
30 strong degradation induced by volcanic/thermal and aqueous processes might explain why we did not  
31 observe phytol, or much archaeal membrane isoprenoids, steroids, hopanoids, and other terpenoids  
32 [113-116]. The second reason for the absence of detection is the MS detection limits for these  
33 compounds and the low number of archaeal cells per mL (between 10<sup>3</sup> and 10<sup>5</sup> cells mL<sup>-1</sup>). These  
34 isoprenoids similar to proteins are complex biosignatures that involve energetic and time-consuming  
35 production processes enhanced by catalytic metabolisms. Hence, they might not be detected  
36 abiotically, which is confirmed by the absence of detection in meteorites and returned samples. To  
37 detect these biotic-driven molecules, the quantity of cells in collected extraterrestrial samples should  
38 be higher than 10<sup>5</sup> cells mL<sup>-1</sup> for MS detection by pyrolysis or thermochemolysis [147].

39 Biomolecules/by-products as a whole (that are not produced abiotically) might represent a  
40 "biosignature", which could reveal the presence of primitive archaea and/or gram-positive bacteria in  
41 extraterrestrial samples, since they are both the main populations in hydrothermal systems and what  
42 we think as being the first populations on the Early-Earth (Euryarchaeota, DPANN, and likely Asgard  
43 and TACK superphyla) [148,149]. The lipid content was similar in all samples except for diethers,  
44 sterols, GDGTs, glycolipids, and sugars. We also found biomolecules that have different metabolic  
45 roles, such as N-(2-acetamido)iminodiacetic acid (cellular buffer), amino acids (protein bases and  
46 secondary metabolites), nucleobases (DNA and RNA bases), and S-bearing compounds like  
47 carbonimidodithioic acid, methyl- (that might be secondary metabolite products). In pyrolysis at 600  
48 °C, we also observed the degradation of all microbial metabolites with alkanes and alkenes ranging

1 from C<sub>10</sub> to C<sub>20-22</sub> (with a greater abundance from C<sub>16</sub> to C<sub>20</sub> from bacterial populations) with an even-  
2 over-odd predominance. Indeed, odd organic compounds ranged only between C<sub>15</sub> and C<sub>23</sub> two to ten  
3 times lower in abundance compared to the even compounds. This even-over-odd predominance has  
4 been observed for alkanes, alkenes, and methylated fatty acids in TMAH and TMSH experiments. This  
5 disruptive length of skeleton carbons is related to Earth life microbes that favored mid-chain lipids for  
6 robustness and adaptive selection to achieve osmotic balance, inter and intra-population  
7 communication or quorum sensing, and nutrients absorption. We identified monomethyl alkanes (*e.g.*,  
8 n-nonomethylhexadecane and n-monomethylheptadecane) like in previous Yellowstone hot springs  
9 that recorded the presence of cyanobacteria [150], and longer-chain fatty acids and saturated  
10 components are more abundant at higher temperatures consistent with literature for thermostability  
11 and/or acidophilic metabolisms for osmotic equilibrium and preserve a neutral-alkaline state in cells  
12 to have phosphate and other nutrients at the base state [90,145,151].  
13

14 Hence, the metabolites segregated three different communities for the three different hot  
15 springs due primarily to temperature and pH of the distal apron sinters collected: i) (hyper-  
16 )thermophiles' community in the 'Similar geyser' (SG Dig) hot-spring with numerous ether bonds (*e.g.*,  
17 octanoic acid, methoxy-, 8-dodecenoic acid, methoxy-, and hexadecanoic acid, methoxy-) belonging to  
18 archaeal membranes and few bacterial domains of life (such as *Aquificales* [32,105]) including dialkyl  
19 glycerol diethers (DGDs) and dialkyl glycerol tetraethers (GDGTs) for membrane stabilization in hot  
20 waters [98,106,107], ii) mesophiles, thermotolerants, and acidophiles form a community in the  
21 'Goldilocks' (GI Dig), and iii) neutrophile to alkaliphile thermophilic populations at Dante's Inferno  
22 (DI Active and DI Old) hot springs, presenting specific features, such as monomethyl and long-chain  
23 unsaturated alkanes and alkenes (from *Chloroflexi* [108–110]), linear isoprenoids (from *Cyanobacteria*  
24 [111–113]), and by-products of pigments for bacterial and oxygenic phototrophs (where symbiotic  
25 association between *Cyanobacteria* and *Chloroflexi* within collected microbial mats).

**Table 4.** Populations identified based on the lipidic and by-product metabolomic study performed in GC-MS (pyrolysis, TMAH and TMSH thermochemolysis).

	Metabolites or biochemical families	Domain of life	Environmental adaptations
Lipids	FAMEs (>C23)	Few in all three	/
	FAMEs (<C23)	All three	/
	Unsaturated FAMEs	Eukaryote (and bacteria and archaea if monounsaturated)	Desaturases that elongate and desaturate saturated fatty acids: allow using free fatty acids by extracellular supply (1). The polyunsaturated fatty acids have important structural roles in cell membranes formation and integrity, but also physiology and signaling mechanisms (3). They are also intermediates in biologically active molecules synthesis (e.g., eicosanoids). Moreover, algae can produce the unsaturated acids by an aerobic and an anaerobic pathways, which is useful in extreme salty environments where water activity and oxygen content fluctuate according to the season. In our hot-springs, the anaerobic condition can be useful for algae being trapped in deep sinters (2). These are mostly useful for organelles in eukaryotes.
	(odd) Straight-chain FAMEs (fatty acids and fatty alcohols)	Eukaryote (and bacteria if <C23)	/
	Isoprenoid	Archaea	Extreme environments, especially halophiles for osmotic exchange and balance.
	Triglycerid	Eukaryotes	All for metabolic energy reserves.
	Fatty-acyl and diacylglycerol	Bacteria	/
	Diether phytanol-glycerol, archeol	Archaea primarily	Resistance to salty, highly thermal, and acidic biotopes, but do not synthesize fatty acids compared all other organisms to produce lipid membranes.
	Cyclopropane ring	Bacteria and few eukaryotes	/
	Phytol hydrolysis	All three	Resistance to specific environments and use of light for energetic metabolism.
Isoprenoid from pigments (chlorophyll, carotenoid)			
Sterols		Eukaryotes primarily and few bacteria	For membrane and eukaryotic organelles.
PAHs		Bacteria and eukaryotes primarily	By-products from lipid membrane, pigments.

Alkanes	Monomethyl	Bacteria	Cyanobacteria synthesize hydrocarbons through enzymatic modification of an elongated fatty acid (Coates et al., 2014). C17 n-alkane is specific to cyanobacteria branch.
Unsaturated compounds		Bacteria and eukaryotes	Thermophilic-metabolism.
S-compounds		All three	Sulfur-metabolism .
Phenol		Bacteria	Thermophilic-metabolism.
Polysaccharide		All three	Glyceraldehyde is reduced in glycerol that can be used for triglyceraldehyde stored in droplet form as metabolic energy reserves by bacteria and eukaryotes.
Hopanoid and steroid		Prokaryote and eukaryote, respectively	Rigidify the membrane for thermal resistance.

---

\* few gram negative found in hot springs similar to Yellowstone Acidobacteriota, Aquificae, Bacteroidetes, Chloroflexia, Cyanobacteria, Pseudomonadota

\*\* few gram positive have been found in similar Yellowstone samples to our hot springs: Actinomycetota

\*\*\* few thermoacidophiles have been found in similar Yellowstone samples to our hot springs:

(Thermoproteota and Thermoprotei orders) and Euryarchaeota archaeal branch, and Cyanidiales-Crenarchaeota archaeplastida eukaryote

## V. Conclusions

Mars has been visited multiple times at multiple locations representing different types of environments. The future explorations by the Mars rovers of ancient volcanic systems may give clues to detect complex and heavy organic compounds on Mars. Silica sinters preserve organic matter and fossils from UV radiation over a long period of time (millions to billions of years). In addition, volcanic systems are full of features and specific signatures that are preserved over billions of years after the inactivity of the system. Therefore, to predict the type of bioindicators, biosignatures, or geophysical features we are looking for on Mars, we visited Mars analog volcanic-hydrothermal systems. Three sites across Yellowstone National Park (WY, USA) were selected for sampling based on criteria of temperature (above and below the upper limit for photosynthesis and microalgae survival, *i.e.*, 72 °C), pH (acidic to alkaline), and low to very low biomass (from 0.1 to 1 % in TOC by dry weight) for Mars relevance according to the different past very active volcanic areas observed and/or explored by rovers/landers (Viking, Spirit, Phoenix, Curiosity, Perseverance, and in the future Rosalind Franklin). We confirmed previous results observed in other studies that primarily lipid biomarkers are well preserved in geothermal sinters due to a rapid silicification [32,142,143,152].

The different signatures detected across the study can be gathered into three groups: i) the geophysical linked to geobiological features (*i.e.*, pyrite associated to biofilm or degraded EPS molecules; ii) the geochemical signatures (*i.e.*, correlation of uncommon isotopy for carbon, nitrogen, and sulfur compared to the average isotopic ratio on Mars); correlation between the concentration in organic matter and specific elements such as sulfates, carbonates, arsenic, cesium; and iii) degraded or intact heavy molecular organic compounds such as PAHs, alkanes, and lipids, sugars and alcohols, amino acids and amines; a ratio  $C_{24}-C_{30}/C_{1}-C_{20}$  equivalent to Mars analog found in Yellowstone and on Earth volcanic systems; the degraded pattern and compounds of lipids relative to the one known on Earth after few million to billions of years. We can extrapolate to all hot spring systems on Earth and potentially to Mars that we have three types of communities according to the range of temperature and pH: i) acidophilic and (hyper)thermophilic communities constituted mostly by *Chloroflexi*, *Actinobacteria*, *Sulfolobales*, *Geoarchaeales*, and few populations of sulfo-oxidizers (and in the distal-apron sinters oxygenic photosynthesizers like green algae); ii) neutral and ambient temperature with *Proteobacteria*, *Aquificae*, few *Thermoproteales*, and *Desulfurococcales*; and iii) alkaline and (hyper)thermophilic hot springs where chemotrophic and thermophilic populations thrive, notably *Chloroflexi*, *Aquificae*, hyperthermophilic archaea, and in the distal-apron area *Cyanobacteria*, and few fungi, diatoms, oxygenic and anoxic photosynthesizers. Therefore, for future Mars explorations and return sample analysis we should investigate the molecular and potentially microbial signatures connected to these populations.

There were robust microbial communities living in and on the siliceous deposits/in the hot springs for each of these environments. Indeed, by comparing siliceous sinters from these different geochemical environments provides evidence for how the extant microbial communities (and/or signals generated by them) are preserved within the silica precipitated at the different sites - which is critical to communicate to the planetary community, since all of the siliceous sinters have physical evidence of life (as well as geochemical). This helps to show that any hot spring siliceous sinter deposit that is found on Mars should absolutely be studied in depth. Therefore, in our Early diagenesis processing samples, we proved the higher preservation rate of microbial communities in acidic environment on the opposite of alkaline hot springs (on the opposite of the first insight and hypothesis we may have where alkaline springs support the production of different minerals that might help the fossilization or preservation of cells like sulfates). The results lead to a second new conclusion that must be verified on further hot springs in Mars analog environments regarding the degradation of past or current life traces in neutral to alkaline silica sinters before diagenesis process meaning the

1 implication of most probably chemical interactions with the organic compounds that degrades faster  
2 or as fast as the diagenesis process. Therefore, on Mars, we should study past and/or present acidic  
3 silica sinters and volcanic sites to detect organic compounds from samples dating back billions of years.  
4

## 5 **Acknowledgment**

6 Accreditation from Yellowstone National park, and the collaborators that help collect samples and  
7 analyze data. A portion of this work was conducted at the Jet Propulsion Laboratory, California Institute  
8 of Technology under a contract with the National Aeronautics and Space Administration  
9 (80NM0018D0004). We also would like to thanks Fulbright for the Student-Research grant. And we  
10 thank the scientists in UF (Jason Curtis, John M. Jaeger, Alison A. Trachet, George Kamenov, Jay Dynes,  
11 Kristy Schepker, and Stephen M. Elardo) and CentraleSupélec-UPS (Pascale Gemeiner). The decision to  
12 implement Mars Sample Return and the Rosalind Franklin rover mission will not be finalized until  
13 NASA's completion of the National Environmental Policy Act (NEPA) process. This document is being  
14 made available for information purposes only.  
15

## 16 **References**

- 17 [1] L.E. Hays et al., Biosignature Preservation and Detection in Mars Analog Environments,  
18 *Astrobiology* 17 (2017) 363–400. <https://doi.org/10.1089/ast.2016.1627>.
- 19 [2] A. Corpolongo et al., SHERLOC Raman Mineral Class Detections of the Mars 2020 Crater Floor  
20 Campaign, *Journal of Geophysical Research: Planets* 128 (2023) e2022JE007455.  
21 <https://doi.org/10.1029/2022JE007455>.
- 22 [3] L.E. Hays, *NASA Astrobiology Strategy 2015*, (2015).
- 23 [4] K. Biemann, On the ability of the Viking gas chromatograph–mass spectrometer to detect  
24 organic matter, *Proceedings of the National Academy of Sciences* 104 (2007) 10310–10313.  
25 <https://doi.org/10.1073/pnas.0703732104>.
- 26 [5] P.T. Palmer, T.F. Limer, Mass spectrometry in the U.S. space program: Past, present, and  
27 future, *J. Am. Soc. Mass Spectrom.* 12 (2001) 656–675. [https://doi.org/10.1016/S1044-](https://doi.org/10.1016/S1044-0305(01)00249-5)  
28 [0305\(01\)00249-5](https://doi.org/10.1016/S1044-0305(01)00249-5).
- 29 [6] H.P. Klein, J. Lederberg, A. Rich, N.H. Horowitz, V.I. Oyama, G.V. Levin, The Viking Mission  
30 search for life on Mars, *Nature* 262 (1976) 24–27. <https://doi.org/10.1038/262024a0>.
- 31 [7] K. Biemann et al., The search for organic substances and inorganic volatile compounds in the  
32 surface of Mars, *J. Geophys. Res.* 82 (1977) 4641–4658.  
33 <https://doi.org/10.1029/JS082i028p04641>.
- 34 [8] W.V. Boynton et al., Thermal and Evolved Gas Analyzer: Part of the Mars Volatile and Climate  
35 Surveyor integrated payload, *J. Geophys. Res.* 106 (2001) 17683–17698.  
36 <https://doi.org/10.1029/1999JE001153>.
- 37 [9] P.R. Mahaffy et al., The Sample Analysis at Mars Investigation and Instrument Suite, *Space Sci*  
38 *Rev* 170 (2012) 401–478. <https://doi.org/10.1007/s11214-012-9879-z>.
- 39 [10] P. François et al., Magnesium sulfate as a key mineral for the detection of organic molecules on  
40 Mars using pyrolysis: MG SULFATE EFFECT ON ORGANIC PYROLYSIS, *J. Geophys. Res. Planets*  
41 121 (2016) 61–74. <https://doi.org/10.1002/2015JE004884>.
- 42 [11] D.M. Hassler et al., Mars' surface radiation environment measured with the Mars Science  
43 Laboratory's Curiosity rover, *Science* 343 (2014) 1244797.
- 44 [12] G. Kminek, J. Bada, The effect of ionizing radiation on the preservation of amino acids on Mars,  
45 *Earth and Planetary Science Letters* 245 (2006) 1–5.  
46 <https://doi.org/10.1016/j.epsl.2006.03.008>.

- 1 [13] A.A. Pavlov, G. Vasilyev, V.M. Ostryakov, A.K. Pavlov, P. Mahaffy, Degradation of the organic  
2 molecules in the shallow subsurface of Mars due to irradiation by cosmic rays: ORGANIC  
3 MATTER AND COSMIC RAYS ON MARS, *Geophys. Res. Lett.* 39 (2012) n/a-n/a.  
4 <https://doi.org/10.1029/2012GL052166>.
- 5 [14] J.P. Grotzinger et al., Mars Science Laboratory Mission and Science Investigation, *Space Sci Rev*  
6 170 (2012) 5–56. <https://doi.org/10.1007/s11214-012-9892-2>.
- 7 [15] J. Grotzinger, Z. Al-Rawahi, Depositional facies and platform architecture of microbialite-  
8 dominated carbonate reservoirs, Ediacaran–Cambrian Ara Group, Sultanate of Oman, *AAPG*  
9 *Bulletin* 98 (2014) 1453–1494. <https://doi.org/10.1306/02271412063>.
- 10 [16] J. L’Haridon et al., Iron Mobility During Diagenesis at Vera Rubin Ridge, Gale Crater, Mars,  
11 *Journal of Geophysical Research: Planets* 125 (2020) e2019JE006299.  
12 <https://doi.org/10.1029/2019JE006299>.
- 13 [17] B.L. Carrier, S.P. Kounaves, The origins of perchlorate in the Martian soil, *Geophys. Res. Lett.* 42  
14 (2015) 3739–3745. <https://doi.org/10.1002/2015GL064290>.
- 15 [18] B.C. Clark, S.P. Kounaves, Evidence for the distribution of perchlorates on Mars, *International*  
16 *Journal of Astrobiology* 15 (2016) 311–318. <https://doi.org/10.1017/S1473550415000385>.
- 17 [19] A. Aubrey et al., Sulfate minerals and organic compounds on Mars, *Geol* 34 (2006) 357.  
18 <https://doi.org/10.1130/G22316.1>.
- 19 [20] J.M.T. Lewis, J.S. Watson, J. Najorka, D. Luong, M.A. Sephton, Sulfate Minerals: A Problem for  
20 the Detection of Organic Compounds on Mars?, *Astrobiology* 15 (2015) 247–258.  
21 <https://doi.org/10.1089/ast.2014.1160>.
- 22 [21] M.C. Casero, C. Ascaso, A. Quesada, H. Mazur-Marzec, J. Wierzbos, Response of Endolithic  
23 *Chroococciopsis* Strains From the Polyextreme Atacama Desert to Light Radiation, *Frontiers in*  
24 *Microbiology* 11 (2021). <https://www.frontiersin.org/articles/10.3389/fmicb.2020.614875>.
- 25 [22] A. Crits-Christoph et al., Colonization patterns of soil microbial communities in the Atacama  
26 Desert, *Microbiome* 1 (2013) 28. <https://doi.org/10.1186/2049-2618-1-28>.
- 27 [23] R. Navarro-Gonzalez, Mars-Like Soils in the Atacama Desert, Chile, and the Dry Limit of  
28 Microbial Life, *Science* 302 (2003) 1018–1021. <https://doi.org/10.1126/science.1089143>.
- 29 [24] M.B. Wilhelm et al., Xeropreservation of functionalized lipid biomarkers in hyperarid soils in the  
30 Atacama Desert, *Organic Geochemistry* 103 (2017) 97–104.  
31 <https://doi.org/10.1016/j.orggeochem.2016.10.015>.
- 32 [25] E.L. Scheller et al., Aqueous alteration processes in Jezero crater, Mars—implications for  
33 organic geochemistry, *Science* 378 (2022) 1105–1110.
- 34 [26] N. Mangold et al., Fluvial Regimes, Morphometry, and Age of Jezero Crater Paleolake Inlet  
35 Valleys and Their Exobiological Significance for the 2020 Rover Mission Landing Site,  
36 *Astrobiology* 20 (2020) 994–1013. <https://doi.org/10.1089/ast.2019.2132>.
- 37 [27] T.A. Goudge, R.E. Milliken, J.W. Head, J.F. Mustard, C.I. Fassett, Sedimentological evidence for a  
38 deltaic origin of the western fan deposit in Jezero crater, Mars and implications for future  
39 exploration, *Earth and Planetary Science Letters* 458 (2017) 357–365.  
40 <https://doi.org/10.1016/j.epsl.2016.10.056>.
- 41 [28] K.M. Stack-Morgan et al., Sedimentology And Stratigraphy Of The Lower Delta Sequence,  
42 Jezero Crater, Mars, in: 54th Lunar and Planetary Science Conference, Lunar and Planetary  
43 Institute, The Woodlands (Texas), United States, 2023: p. 1422. [https://hal.science/hal-](https://hal.science/hal-04052338)  
44 [04052338](https://hal.science/hal-04052338) (accessed September 11, 2023).
- 45 [29] S.C. Schon, J.W. Head, C.I. Fassett, An overfilled lacustrine system and progradational delta in  
46 Jezero crater, Mars: Implications for Noachian climate, *Planetary and Space Science* 67 (2012)  
47 28–45. <https://doi.org/10.1016/j.pss.2012.02.003>.
- 48 [30] J.L. Eigenbrode et al., Organic matter preserved in 3-billion-year-old mudstones at Gale crater,  
49 Mars, *Science* 360 (2018) 1096–1101. <https://doi.org/10.1126/science.aas9185>.
- 50 [31] S.R. Gainey et al., Clay mineral formation under oxidized conditions and implications for  
51 paleoenvironments and organic preservation on Mars, *Nat Commun* 8 (2017) 1230.  
52 <https://doi.org/10.1038/s41467-017-01235-7>.

- 1 [32] R.D. Pancost, S. Pressley, J.M. Coleman, L.G. Benning, B.W. Mountain, Lipid biomolecules in  
2 silica sinters: indicators of microbial biodiversity, *Environmental Microbiology* 7 (2005) 66–77.  
3 <https://doi.org/10.1111/j.1462-2920.2004.00686.x>.
- 4 [33] S. Sharma et al., Diverse organic-mineral associations in Jezero crater, Mars, *Nature* (2023) 1–9.
- 5 [34] F. Goesmann et al., The Mars Organic Molecule Analyzer (MOMA) Instrument: Characterization  
6 of Organic Material in Martian Sediments, *Astrobiology* 17 (2017) 655–685.  
7 <https://doi.org/10.1089/ast.2016.1551>.
- 8 [35] P. Fawdon et al., The high-resolution map of Oxia Planum, Mars; the landing site of the  
9 ExoMars Rosalind Franklin rover mission, *Journal of Maps* (2024) 20(1).  
10 <https://doi.org/10.1080/17445647.2024.2302361>.
- 11 [36] S. Alwmark et al., Diverse lava flow morphologies in the stratigraphy of the Jezero Crater Floor,  
12 *Journal of Geophysical Research. Planets* (2023) e2022JE007446.
- 13 [37] A.J. Brown, C.E. Viviano, T.A. Goudge, Olivine-carbonate mineralogy of the Jezero crater region,  
14 *Journal of Geophysical Research: Planets* 125 (2020) e2019JE006011.
- 15 [38] J.L. Vago et al., Habitability on Early Mars and the Search for Biosignatures with the ExoMars  
16 Rover, *Astrobiology* 17 (2017) 471–510. <https://doi.org/10.1089/ast.2016.1533>.
- 17 [39] D.M. Hassler et al., Mars' Surface Radiation Environment Measured with the Mars Science  
18 Laboratory's Curiosity Rover, *Science* 343 (2014) 1244797.  
19 <https://doi.org/10.1126/science.1244797>.
- 20 [40] W. Goetz et al., MOMA: the challenge to search for organics and biosignatures on Mars,  
21 *International Journal of Astrobiology* 15 (2016) 239–250.  
22 <https://doi.org/10.1017/S1473550416000227>.
- 23 [41] O. Abramov, D.A. Kring, Impact-induced hydrothermal activity on early Mars, *Journal of*  
24 *Geophysical Research: Planets* 110 (2005). <https://doi.org/10.1029/2005JE002453>.
- 25 [42] G.R. Osinski et al., Impact-generated hydrothermal systems on Earth and Mars, *Icarus* 224  
26 (2013) 347–363. <https://doi.org/10.1016/j.icarus.2012.08.030>.
- 27 [43] M.H. Carr, *Water On Mars*, Oxford University Press, 1996.  
28 <https://doi.org/10.1093/oso/9780195099386.001.0001>.
- 29 [44] S.W. Squyres et al., Detection of Silica-Rich Deposits on Mars, *Science* 320 (2008) 1063–1067.  
30 <https://doi.org/10.1126/science.1155429>.
- 31 [45] S.W. Ruff et al., Characteristics, distribution, origin, and significance of opaline silica observed  
32 by the Spirit rover in Gusev crater, Mars, *Journal of Geophysical Research: Planets* 116 (2011).  
33 <https://doi.org/10.1029/2010JE003767>.
- 34 [46] J. Frydenvang et al., Diagenetic silica enrichment and late-stage groundwater activity in Gale  
35 crater, Mars, *Geophysical Research Letters* 44 (2017) 4716–4724.  
36 <https://doi.org/10.1002/2017GL073323>.
- 37 [47] M. Golombek et al., Selection of the Mars Science Laboratory Landing Site, *Space Sci Rev* 170  
38 (2012) 641–737. <https://doi.org/10.1007/s11214-012-9916-y>.
- 39 [48] T. Djokic, M.J. Van Kranendonk, K.A. Campbell, M.R. Walter, C.R. Ward, Earliest signs of life on  
40 land preserved in ca. 3.5 Ga hot spring deposits, *Nat Commun* 8 (2017) 15263.  
41 <https://doi.org/10.1038/ncomms15263>.
- 42 [49] C. Gillen, C. Jeancolas, S. McMahon, P. Vickers, The Call for a New Definition of Biosignature,  
43 *Astrobiology* 23 (2023) 1228–1237. <https://doi.org/10.1089/ast.2023.0010>.
- 44 [50] M.J. Mumma et al., Strong Release of Methane on Mars in Northern Summer 2003, *Science* 323  
45 (2009) 1041–1045. <https://doi.org/10.1126/science.1165243>.
- 46 [51] C.R. Webster et al., Mars methane detection and variability at Gale crater, *Science* 347 (2015)  
47 415–417. <https://doi.org/10.1126/science.1261713>.
- 48 [52] S.J. Knak Jensen et al., A sink for methane on Mars? The answer is blowing in the wind, *Icarus*  
49 236 (2014) 24–27. <https://doi.org/10.1016/j.icarus.2014.03.036>.
- 50 [53] M. Neveu, L.E. Hays, M.A. Voytek, M.H. New, M.D. Schulte, The Ladder of Life Detection,  
51 *Astrobiology* 18 (2018) 1375–1402. <https://doi.org/10.1089/ast.2017.1773>.

- 1 [54] O. Prieto-Ballesteros, J.S. Kargel, A.G. Fairén, D.C. Fernández-Remolar, J.M. Dohm, R. Amils,  
2 Interglacial clathrate destabilization on Mars: Possible contributing source of its atmospheric  
3 methane, *Geology* 34 (2006) 149–152. <https://doi.org/10.1130/G22311.1>.
- 4 [55] S.R. Gainey, M.E. Elwood Madden, Kinetics of methane clathrate formation and dissociation  
5 under Mars relevant conditions, *Icarus* 218 (2012) 513–524.  
6 <https://doi.org/10.1016/j.icarus.2011.12.019>.
- 7 [56] J. Carter, L. Riu, F. Poulet, J.-P. Bibring, Y. Langevin, B. Gondet, A Mars orbital catalog of  
8 aqueous alteration signatures (MOCAAS), *Icarus* 389 (2023) 115164.
- 9 [57] J. Carter, C. Quantin, P. Thollot, D. Loizeau, A. Ody, L. Lozach, Oxia Planum: A Clay-Laden  
10 Landing Site Proposed for the ExoMars Rover Mission: Aqueous Mineralogy and Alteration  
11 Scenarios, (2016) 2064.
- 12 [58] A. Williams et al., Results from the TMAH Wet Chemistry Experiment on the Sample Analysis at  
13 Mars (SAM) Instrument Onboard NASA’s Curiosity Rover, 43 (2021) 1939.
- 14 [59] A.C. McAdam et al., Sulfur-bearing phases detected by evolved gas analysis of the Rocknest  
15 aeolian deposit, Gale Crater, Mars: ROCKNEST SULFUR PHASES DETECTED BY SAM, *J. Geophys.*  
16 *Res. Planets* 119 (2014) 373–393. <https://doi.org/10.1002/2013JE004518>.
- 17 [60] H.B. Franz et al., Large sulfur isotope fractionations in Martian sediments at Gale crater, *Nature*  
18 *Geosci* 10 (2017) 658–662. <https://doi.org/10.1038/ngeo3002>.
- 19 [61] K.E. Miller, J.L. Eigenbrode, C. Freissinet, D.P. Glavin, B. Kotrc, P. Francois, R.E. Summons,  
20 Potential precursor compounds for chlorohydrocarbons detected in Gale Crater, Mars, by the  
21 SAM instrument suite on the Curiosity Rover: Precursors Of Martian Chlorohydrocarbons, *J.*  
22 *Geophys. Res. Planets* 121 (2016) 296–308. <https://doi.org/10.1002/2015JE004939>.
- 23 [62] C. Szopa et al., First Detections of Dichlorobenzene Isomers and Trichloromethylpropane from  
24 Organic Matter Indigenous to Mars Mudstone in Gale Crater, Mars: Results from the Sample  
25 Analysis at Mars Instrument Onboard the Curiosity Rover, *Astrobiology* 20 (2020) 292–306.  
26 <https://doi.org/10.1089/ast.2018.1908>.
- 27 [63] C. Freissinet et al., Organic molecules in the Sheepbed Mudstone, Gale Crater, Mars: Detection  
28 of organics in martian sample, *J. Geophys. Res. Planets* 120 (2015) 495–514.  
29 <https://doi.org/10.1002/2014JE004737>.
- 30 [64] J. Clark et al., A Review of Sample Analysis at Mars-Evolved Gas Analysis Laboratory Analog  
31 Work Supporting the Presence of Perchlorates and Chlorates in Gale Crater, Mars, *Minerals* 11  
32 (2021) 475. <https://doi.org/10.3390/min11050475>.
- 33 [65] P.D. Archer et al., Abundances and implications of volatile-bearing species from evolved gas  
34 analysis of the Rocknest aeolian deposit, Gale Crater, Mars, *J. Geophys. Res. Planets* 119 (2014)  
35 237–254. <https://doi.org/10.1002/2013JE004493>.
- 36 [66] D.P. Glavin et al., Evidence for perchlorates and the origin of chlorinated hydrocarbons  
37 detected by SAM at the Rocknest aeolian deposit in Gale Crater: Evidence For Perchlorates At  
38 Rocknest, *J. Geophys. Res. Planets* 118 (2013) 1955–1973. <https://doi.org/10.1002/jgre.20144>.
- 39 [67] C. Freissinet et al., Detection of Long-Chain Hydrocarbons on Mars with the Sample Analysis at  
40 Mars (SAM) Instrument, 2089 (2019) 6123.
- 41 [68] M.C. Pietrogrande, D. Bacco, S. Chiereghin, GC/MS analysis of water-soluble organics in  
42 atmospheric aerosol: optimization of a solvent extraction procedure for simultaneous analysis  
43 of carboxylic acids and sugars, *Anal Bioanal Chem* 405 (2013) 1095–1104.  
44 <https://doi.org/10.1007/s00216-012-6592-4>.
- 45 [69] A. Buch et al., Influence of the secondary X-Rays on the organic matter at Mars’ near-surface,  
46 AGU Fall Meeting Abstracts 2022 (2022) P12A-08.
- 47 [70] R. dos Santos, M. Patel, J. Cuadros, Z. Martins, Influence of mineralogy on the preservation of  
48 amino acids under simulated Mars conditions, *Icarus* 277 (2016) 342–353.  
49 <https://doi.org/10.1016/j.icarus.2016.05.029>.
- 50 [71] J.R. Havig, J.E. Kuether, A.J. Gangidine, S. Schroeder, T.L. Hamilton, Hot Spring Microbial  
51 Community Elemental Composition: Hot Spring and Soil Inputs, and the Transition from

- 1 Biocumulus to Siliceous Sinter, *Astrobiology* 21 (2021) 1526–1546.  
2 <https://doi.org/10.1089/ast.2019.2086>.
- 3 [72] R. Navarro-Gonzalez et al., The limitations on organic detection in Mars-like soils by thermal  
4 volatilization-gas chromatography-MS and their implications for the Viking results, *Proceedings*  
5 *of the National Academy of Sciences* 103 (2006) 16089–16094.  
6 <https://doi.org/10.1073/pnas.0604210103>.
- 7 [73] K.A. Campbell, D.M. Guido, P. Gautret, F. Foucher, C. Ramboz, F. Westall, Geyselite in hot-  
8 spring siliceous sinter: Window on Earth's hottest terrestrial (paleo)environment and its  
9 extreme life, *Earth-Science Reviews* 148 (2015) 44–64.  
10 <https://doi.org/10.1016/j.earscirev.2015.05.009>.
- 11 [74] A. Gangidine, J.R. Havig, D.A. Fike, C. Jones, T.L. Hamilton, A.D. Czaja, Trace Element  
12 Concentrations in Hydrothermal Silica Deposits as a Potential Biosignature, *Astrobiology* 20  
13 (2020) 525–536. <https://doi.org/10.1089/ast.2018.1994>.
- 14 [75] B.L. Teece, J.R. Havig, S.C. George, T.L. Hamilton, R.J. Baumgartner, J. Hartz, M.J. Van  
15 Kranendonk, Biogeochemistry of Recently Fossilized Siliceous Hot Spring Sinters from  
16 Yellowstone, USA, *Astrobiology* 23 (2023) 155–171. <https://doi.org/10.1089/ast.2022.0012>.
- 17 [76] B.L. Teece, D.M. Guido, K.A. Campbell, M.J. Van Kranendonk, A. Galar, S.C. George, Exceptional  
18 molecular preservation in the Late Jurassic Claudia palaeo-geothermal field (Deseado Massif,  
19 Patagonia, Argentina), *Organic Geochemistry* 173 (2022) 104504.  
20 <https://doi.org/10.1016/j.orggeochem.2022.104504>.
- 21 [77] M. Gonsior, N. Hertkorn, N. Hinman, S.E.-M. Dvorski, M. Harir, W.J. Cooper, P. Schmitt-Kopplin,  
22 Yellowstone Hot Springs are Organic Chemodiversity Hot Spots, *Sci Rep* 8 (2018) 14155.  
23 <https://doi.org/10.1038/s41598-018-32593-x>.
- 24 [78] P.L. Finkel, D. Carrizo, V. Parro, L. Sánchez-García, An Overview of Lipid Biomarkers in  
25 Terrestrial Extreme Environments with Relevance for Mars Exploration, *Astrobiology* 23 (2023)  
26 563–604. <https://doi.org/10.1089/ast.2022.0083>.
- 27 [79] T.L. Hamilton, A.C. Bennett, S.K. Murugapiran, J.R. Havig, Anoxygenic Phototrophs Span  
28 Geochemical Gradients and Diverse Morphologies in Terrestrial Geothermal Springs, *mSystems*  
29 4 (2019) 10.1128/msystems.00498-19. <https://doi.org/10.1128/msystems.00498-19>.
- 30 [80] J.R. Havig, T.L. Hamilton, Hypolithic Photosynthesis in Hydrothermal Areas and Implications for  
31 Cryptic Oxygen Oases on Archean Continental Surfaces, *Frontiers in Earth Science* 7 (2019).  
32 <https://www.frontiersin.org/articles/10.3389/feart.2019.00015>.
- 33 [81] S. Hurwitz, J.B. Lowenstern, Dynamics of the Yellowstone hydrothermal system, *Reviews of*  
34 *Geophysics* 52 (2014) 375–411. <https://doi.org/10.1002/2014RG000452>.
- 35 [82] H.A. Waldrop, K.L. Pierce, Surficial geologic map of the Madison Junction Quadrangle,  
36 Yellowstone National Park, Wyoming, *IMAP* (1975). <https://doi.org/10.3133/i651>.
- 37 [83] J.R. Havig, T.L. Hamilton, Productivity and Community Composition of Low Biomass/High Silica  
38 Precipitation Hot Springs: A Possible Window to Earth's Early Biosphere?, *Life* 9 (2019) 64.  
39 <https://doi.org/10.3390/life9030064>.
- 40 [84] M.W. Loewen, I.N. Bindeman, Oxygen isotope thermometry reveals high magmatic  
41 temperatures and short residence times in Yellowstone and other hot-dry rhyolites compared  
42 to cold-wet systems, *American Mineralogist* 101 (2016) 1222–1227.  
43 <https://doi.org/10.2138/am-2016-5591>.
- 44 [85] I.N. Bindeman, J.W. Valley, Formation of low- $\delta^{18}\text{O}$  rhyolites after caldera collapse at  
45 Yellowstone, Wyoming, USA, *Geology* 28 (2000) 719–722. [https://doi.org/10.1130/0091-7613\(2000\)28<719:FOLRAC>2.0.CO;2](https://doi.org/10.1130/0091-7613(2000)28<719:FOLRAC>2.0.CO;2).
- 46 [86] M.C. Hanson, C. Oze, C. Werner, T.W. Horton, Soil  $\delta^{13}\text{C}$ -CO<sub>2</sub> and CO<sub>2</sub> flux in the H<sub>2</sub>S-rich  
47 Rotorua Hydrothermal System utilizing Cavity Ring Down Spectroscopy, *Journal of Volcanology*  
48 *and Geothermal Research* 358 (2018) 252–260.  
49 <https://doi.org/10.1016/j.jvolgeores.2018.05.018>.
- 50

- 1 [87] J.R. Havig, J. Raymond, D.R. Meyer-Dombard, N. Zolotova, E.L. Shock, Merging isotopes and  
2 community genomics in a siliceous sinter-depositing hot spring, *Journal of Geophysical*  
3 *Research: Biogeosciences* 116 (2011). <https://doi.org/10.1029/2010JG001415>.
- 4 [88] F. Rull, M. Veneranda, J.A. Manrique-Martinez, A. Sanz-Arranz, J. Saiz, J. Medina, A. Moral, C.  
5 Perez, L. Seoane, E. Lalla, E. Charro, J.M. Lopez, L.M. Nieto, G. Lopez-Reyes, Spectroscopic study  
6 of terrestrial analogues to support rover missions to Mars – A Raman-centred review, *Analytica*  
7 *Chimica Acta* 1209 (2022) 339003. <https://doi.org/10.1016/j.aca.2021.339003>.
- 8 [89] Y.B. Zeng, D.M. Ward, S.C. Brassell, G. Eglinton, Biogeochemistry of hot spring environments: 2.  
9 Lipid compositions of Yellowstone (Wyoming, U.S.A.) cyanobacterial and Chloroflexus mats,  
10 *Chemical Geology* 95 (1992) 327–345. [https://doi.org/10.1016/0009-2541\(92\)90020-6](https://doi.org/10.1016/0009-2541(92)90020-6).
- 11 [90] J. Harwood, *Lipids in Plants and Microbes*, Springer Science & Business Media, 2012.
- 12 [91] G. Gago, L. Diacovich, A. Arabolaza, S.-C. Tsai, H. Gramajo, Fatty acid biosynthesis in  
13 actinomycetes, *FEMS Microbiol Rev* 35 (2011) 475–497. [https://doi.org/10.1111/j.1574-](https://doi.org/10.1111/j.1574-6976.2010.00259.x)  
14 [6976.2010.00259.x](https://doi.org/10.1111/j.1574-6976.2010.00259.x).
- 15 [92] P. Kumari, M. Kumar, C.R.K. Reddy, B. Jha, 3 - Algal lipids, fatty acids and sterols, in: H.  
16 Domínguez (Ed.), *Functional Ingredients from Algae for Foods and Nutraceuticals*, Woodhead  
17 Publishing, 2013: pp. 87–134. <https://doi.org/10.1533/9780857098689.1.87>.
- 18 [93] W. Hewelt-Belka, Á. Kot-Wasik, P. Tamagnini, P. Oliveira, Untargeted Lipidomics Analysis of the  
19 Cyanobacterium *Synechocystis* sp. PCC 6803: Lipid Composition Variation in Response to  
20 Alternative Cultivation Setups and to Gene Deletion, *Int J Mol Sci* 21 (2020) 8883.  
21 <https://doi.org/10.3390/ijms21238883>.
- 22 [94] L.S. Passos, P.N.N. de Freitas, R.B. Menezes, A.O. de Souza, M.F. da Silva, A. Converti, E. Pinto,  
23 Content of Lipids, Fatty Acids, Carbohydrates, and Proteins in Continental Cyanobacteria: A  
24 Systematic Analysis and Database Application, *Applied Sciences* 13 (2023) 3162.  
25 <https://doi.org/10.3390/app13053162>.
- 26 [95] D.N. Carruthers, T.S. Lee, Diversifying Isoprenoid Platforms via Atypical Carbon Substrates and  
27 Non-model Microorganisms, *Frontiers in Microbiology* 12 (2021).
- 28 [96] A.O. Chatzivasileiou, V. Ward, S.M. Edgar, G. Stephanopoulos, Two-step pathway for isoprenoid  
29 synthesis, *Proc Natl Acad Sci U S A* 116 (2019) 506–511.  
30 <https://doi.org/10.1073/pnas.1812935116>.
- 31 [97] Y. Koga, H. Morii, Recent Advances in Structural Research on Ether Lipids from Archaea  
32 Including Comparative and Physiological Aspects, *Bioscience, Biotechnology, and Biochemistry*  
33 69 (2005) 2019–2034. <https://doi.org/10.1271/bbb.69.2019>.
- 34 [98] Y. Koga, Thermal Adaptation of the Archaeal and Bacterial Lipid Membranes, *Archaea* 2012  
35 (2012) 789652. <https://doi.org/10.1155/2012/789652>.
- 36 [99] L. Tomečková, A. Tomčala, M. Oborník, V. Hampl, The Lipid Composition of *Euglena gracilis*  
37 Middle Plastid Membrane Resembles That of Primary Plastid Envelopes1, *Plant Physiol* 184  
38 (2020) 2052–2063. <https://doi.org/10.1104/pp.20.00505>.
- 39 [100] A. Vinçon-Laugier, C. Cravo-Laureau, I. Mitteau, V. Grossi, Temperature-Dependent Alkyl  
40 Glycerol Ether Lipid Composition of Mesophilic and Thermophilic Sulfate-Reducing Bacteria,  
41 *Frontiers in Microbiology* 8 (2017).  
42 <https://www.frontiersin.org/articles/10.3389/fmicb.2017.01532>.
- 43 [101] R.J. Lamed, J.G. Zeikus, Novel NADP-linked alcohol–aldehyde/ketone oxidoreductase in  
44 thermophilic ethanologenic bacteria, *Biochemical Journal* 195 (1981) 183–190.  
45 <https://doi.org/10.1042/bj1950183>.
- 46 [102] J.G. Zeikus, A. Ben-Bassat, T.K. Ng, R.J. Lamed, Thermophilic Ethanol Fermentations, in: A.  
47 Hollaender, R. Rabson, P. Rogers, A.S. Pietro, R. Valentine, R. Wolfe (Eds.), *Trends in the Biology*  
48 *of Fermentations for Fuels and Chemicals*, Springer US, Boston, MA, 1981: pp. 441–461.  
49 [https://doi.org/10.1007/978-1-4684-3980-9\\_26](https://doi.org/10.1007/978-1-4684-3980-9_26).
- 50 [103] S.L. Cady, J.D. Farmer, Fossilization Processes in Siliceous Thermal Springs: Trends in  
51 Preservation Along Thermal Gradients, in: *Ciba Foundation Symposium 202 - Evolution of*

- 1 Hydrothermal Ecosystems on Earth (And Mars?), John Wiley & Sons, Ltd, n.d.: pp. 150–173.  
2 <https://doi.org/10.1002/9780470514986.ch9>.
- 3 [104] L.L. Jahnke, W. Eder, R. Huber, J.M. Hope, K.U. Hinrichs, J.M. Hayes, D.J. Des Marais, S.L. Cady,  
4 R.E. Summons, Signature lipids and stable carbon isotope analyses of Octopus Spring  
5 hyperthermophilic communities compared with those of Aquificales representatives, *Appl*  
6 *Environ Microbiol* 67 (2001) 5179–5189. <https://doi.org/10.1128/AEM.67.11.5179-5189.2001>.
- 7 [105] S. Jain, A. Caforio, A.J.M. Driessen, Biosynthesis of archaeal membrane ether lipids, *Frontiers in*  
8 *Microbiology* 5 (2014). <https://www.frontiersin.org/articles/10.3389/fmicb.2014.00641>.
- 9 [106] S.-V. Albers, J.L.C.M. van de Vossen, A.J.M. Driessen, W.N. Konings, Adaptations of the  
10 archaeal cell membrane to heat stress, *FBL* 5 (2000) 813–820. <https://doi.org/10.2741/albers>.
- 11 [107] M.T.J. van der Meer et al., Cultivation and genomic, nutritional, and lipid biomarker  
12 characterization of *Roseiflexus* strains closely related to predominant in situ populations  
13 inhabiting Yellowstone hot spring microbial mats, *J Bacteriol* 192 (2010) 3033–3042.  
14 <https://doi.org/10.1128/JB.01610-09>.
- 15 [108] M.T. van der Meer, S. Schouten, J.W. de Leeuw, D.M. Ward, Autotrophy of green non-sulphur  
16 bacteria in hot spring microbial mats: biological explanations for isotopically heavy organic  
17 carbon in the geological record, *Environ Microbiol* 2 (2000) 428–435.  
18 <https://doi.org/10.1046/j.1462-2920.2000.00124.x>.
- 19 [109] R. Frese, U. Oberheide, I. van Stokkum, R. van Grondelle, M. Foidl, J. Oelze, H. van Amerongen,  
20 The organization of bacteriochlorophyll c in chlorosomes from *Chloroflexus aurantiacus* and the  
21 structural role of carotenoids and protein, *Photosynthesis Research* 54 (1997) 115–126.  
22 <https://doi.org/10.1023/A:1005903613179>.
- 23 [110] H. Goossens, J.W. de Leeuw, P.A. Schenck, S.C. Brassell, Tocopherols as likely precursors of  
24 pristane in ancient sediments and crude oils, *Nature* 312 (1984) 440–442.  
25 <https://doi.org/10.1038/312440a0>.
- 26 [111] B.M. Didyk, B.R.T. Simoneit, S.C. Brassell, G. Eglinton, Organic geochemical indicators of  
27 palaeoenvironmental conditions of sedimentation, *Nature* 272 (1978) 216–222.  
28 <https://doi.org/10.1038/272216a0>.
- 29 [112] M.N. Parenteau, L.L. Jahnke, J.D. Farmer, S.L. Cady, Production and Early Preservation of Lipid  
30 Biomarkers in Iron Hot Springs, *Astrobiology* 14 (2014) 502–521.  
31 <https://doi.org/10.1089/ast.2013.1122>.
- 32 [113] S. Geilert, P.Z. Vroon, N.S. Keller, S. Gudbrandsson, A. Stefánsson, M.J. van Bergen, Silicon  
33 isotope fractionation during silica precipitation from hot-spring waters: Evidence from the  
34 Geysir geothermal field, Iceland, *Geochimica et Cosmochimica Acta* 164 (2015) 403–427.  
35 <https://doi.org/10.1016/j.gca.2015.05.043>.
- 36 [114] S. Geilert, P.Z. Vroon, N.S. Keller, S. Gudbrandsson, A. Stefánsson, M.J. van Bergen, Silicon  
37 isotope fractionation during silica precipitation from hot-spring waters: Evidence from the  
38 Geysir geothermal field, Iceland, *Geochimica et Cosmochimica Acta* 164 (2015) 403–427.  
39 <https://doi.org/10.1016/j.gca.2015.05.043>.
- 40 [115] J.M. Holloway, D.K. Nordstrom, J.K. Böhlke, R.B. McCleskey, J.W. Ball, Ammonium in thermal  
41 waters of Yellowstone National Park: Processes affecting speciation and isotope fractionation,  
42 *Geochimica et Cosmochimica Acta* 75 (2011) 46114636.  
43 <https://doi.org/10.1016/j.gca.2011.05.036>.
- 44 [116] C. Thomazo, D.L. Pinti, V. Busigny, M. Ader, K. Hashizume, P. Philippot, Biological activity and  
45 the Earth's surface evolution: Insights from carbon, sulfur, nitrogen and iron stable isotopes in  
46 the rock record, *Comptes Rendus Palevol* 8 (2009) 665–678.  
47 <https://doi.org/10.1016/j.crpv.2009.02.003>.
- 48 [117] C. Vogel, K. Heister, F. Buegger, I. Tanuwidjaja, S. Haug, M. Schloter, I. Kögel-Knabner, Clay  
49 mineral composition modifies decomposition and sequestration of organic carbon and nitrogen  
50 in fine soil fractions, *Biol Fertil Soils* 51 (2015) 427–442. <https://doi.org/10.1007/s00374-014-0987-7>.
- 51

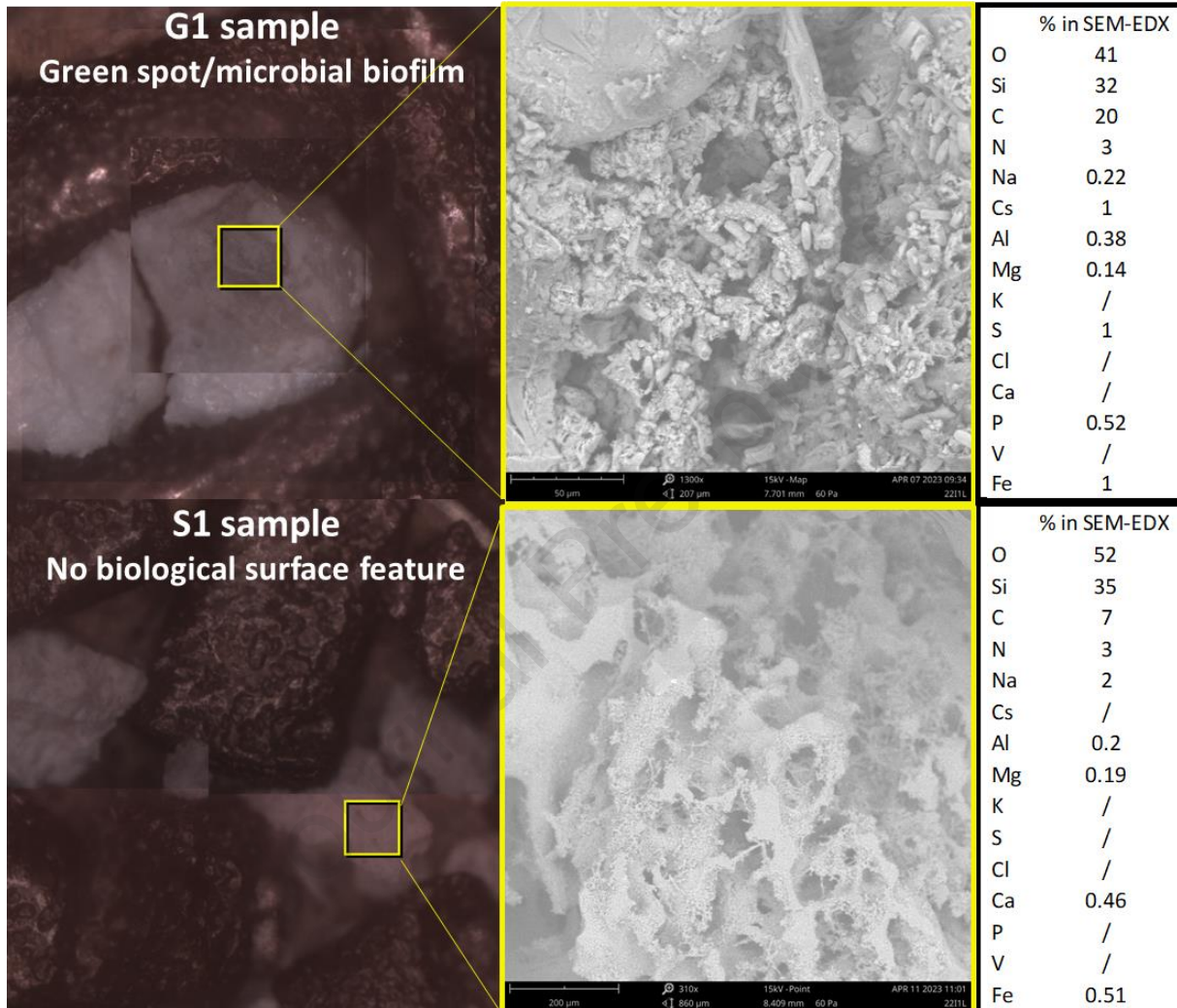
- 1 [118] A. Rimola, M. Sodupe, P. Ugliengo, Role of Mineral Surfaces in Prebiotic Chemical Evolution. In  
2 Silico Quantum Mechanical Studies, *Life* 9 (2019) 10. <https://doi.org/10.3390/life9010010>.
- 3 [119] J. Bundschuh, J.P. Maity, Geothermal arsenic: Occurrence, mobility and environmental  
4 implications, *Renewable and Sustainable Energy Reviews* 42 (2015) 1214–1222.  
5 <https://doi.org/10.1016/j.rser.2014.10.092>.
- 6 [120] R.S. Oremland, J.F. Stolz, The Ecology of Arsenic, *Science* 300 (2003) 939–944.  
7 <https://doi.org/10.1126/science.1081903>.
- 8 [121] B. Jones, Siliceous sinters in thermal spring systems: Review of their mineralogy, diagenesis,  
9 and fabrics, *Sedimentary Geology* 413 (2021) 105820.  
10 <https://doi.org/10.1016/j.sedgeo.2020.105820>.
- 11 [122] A. Darma, J. Yang, E. Bloem, K. Mozdzen, P. Zandi, Arsenic biotransformation and mobilization:  
12 the role of bacterial strains and other environmental variables, *Environ Sci Pollut Res* 29 (2022)  
13 1763–1787. <https://doi.org/10.1007/s11356-021-17117-x>.
- 14 [123] T.M. Gihring, J.F. Banfield, Arsenite oxidation and arsenate respiration by a new *Thermus*  
15 isolate, *FEMS Microbiology Letters* 204 (2001) 335–340. <https://doi.org/10.1111/j.1574-6968.2001.tb10907.x>.
- 16 [124] P.T. Visscher et al., Modern arsenotrophic microbial mats provide an analogue for life in the  
17 anoxic Archean, *Commun Earth Environ* 1 (2020) 1–10. <https://doi.org/10.1038/s43247-020-00025-2>.
- 18 [125] M.C. Sforza et al., Evidence for arsenic metabolism and cycling by microorganisms 2.7 billion  
19 years ago, *Nature Geosci* 7 (2014) 811–815. <https://doi.org/10.1038/ngeo2276>.
- 20 [126] C.G. Schuler, J.R. Havig, T.L. Hamilton, Hot Spring Microbial Community Composition,  
21 Morphology, and Carbon Fixation: Implications for Interpreting the Ancient Rock Record,  
22 *Frontiers in Earth Science* 5 (2017).  
23 <https://www.frontiersin.org/articles/10.3389/feart.2017.00097>.
- 24 [127] L.D. Brabandere, T.K. Frazer, J.P. Montoya, Stable nitrogen isotope ratios of macrophytes and  
25 associated periphyton along a nitrate gradient in two subtropical, spring-fed streams,  
26 *Freshwater Biology* 52 (2007) 1564–1575. <https://doi.org/10.1111/j.1365-2427.2007.01788.x>.
- 27 [128] A.J. Williams et al., Recovery of Fatty Acids from Mineralogic Mars Analogs by TMAH  
28 Thermochemolysis for the Sample Analysis at Mars Wet Chemistry Experiment on the Curiosity  
29 Rover, *Astrobiology* 19 (2019) 522–546. <https://doi.org/10.1089/ast.2018.1819>.
- 30 [129] M. Reinhardt, W. Goetz, V. Thiel, Testing Flight-like Pyrolysis Gas Chromatography–Mass  
31 Spectrometry as Performed by the Mars Organic Molecule Analyzer Onboard the ExoMars 2020  
32 Rover on Oxia Planum Analog Samples, *Astrobiology* 20 (2020) 415–428.  
33 <https://doi.org/10.1089/ast.2019.2143>.
- 34 [130] M. Millan et al., In situ analysis of martian regolith with the SAM experiment during the first  
35 mars year of the MSL mission: Identification of organic molecules by gas chromatography from  
36 laboratory measurements, *Planetary and Space Science* 129 (2016) 88–102.  
37 <https://doi.org/10.1016/j.pss.2016.06.007>.
- 38 [131] M. Millan et al., Organic molecules revealed in Mars’s Bagnold Dunes by Curiosity’s  
39 derivatization experiment, *Nat Astron* 6 (2022) 129–140. <https://doi.org/10.1038/s41550-021-01507-9>.
- 40 [132] J.R. Cronin, S. Pizzarello, S. Epstein, R.V. Krishnamurthy, Molecular and isotopic analyses of the  
41 hydroxy acids, dicarboxylic acids, and hydroxydicarboxylic acids of the Murchison meteorite,  
42 *Geochimica et Cosmochimica Acta* 57 (1993) 4745–4752. [https://doi.org/10.1016/0016-7037\(93\)90197-5](https://doi.org/10.1016/0016-7037(93)90197-5).
- 43 [133] G.U. Yuen, K.A. Kvenvolden, Monocarboxylic Acids in Murray and Murchison Carbonaceous  
44 Meteorites, *Nature* 246 (1973) 301–303. <https://doi.org/10.1038/246301a0>.
- 45 [134] L. Becker, D.P. Glavin, J.L. Bada, Polycyclic aromatic hydrocarbons (PAHs) in Antarctic Martian  
46 meteorites, carbonaceous chondrites, and polar ice, *Geochimica et Cosmochimica Acta* 61  
47 (1997) 475–481. [https://doi.org/10.1016/S0016-7037\(96\)00400-0](https://doi.org/10.1016/S0016-7037(96)00400-0).

- 1 [135] P. Schmitt-Kopplin, Z. Gabelica, R.D. Gougeon, A. Fekete, B. Kanawati, M. Harir, I. Gebefuegi, G.  
2 Eckel, N. Hertkorn, High molecular diversity of extraterrestrial organic matter in Murchison  
3 meteorite revealed 40 years after its fall, *Proceedings of the National Academy of Sciences* 107  
4 (2010) 2763–2768. <https://doi.org/10.1073/pnas.0912157107>.
- 5 [136] A.A. Pavlov, H.L. McLain, D.P. Glavin, A. Roussel, J.P. Dworkin, J.E. Elsila, K.M. Yocum, Rapid  
6 Radiolytic Degradation of Amino Acids in the Martian Shallow Subsurface: Implications for the  
7 Search for Extinct Life, *Astrobiology* (2022) ast.2021.0166.  
8 <https://doi.org/10.1089/ast.2021.0166>.
- 9 [137] A.J. Williams, K.L. Craft, M. Millan, S.S. Johnson, C.A. Knudson, M. Juarez Rivera, A.C. McAdam,  
10 D. Tobler, J.R. Skok, Fatty Acid Preservation in Modern and Relict Hot-Spring Deposits in  
11 Iceland, with Implications for Organics Detection on Mars, *Astrobiology* 21 (2021) 60–82.  
12 <https://doi.org/10.1089/ast.2019.2115>.
- 13 [138] P. Blokker, R. Pel, L. Akoto, U.A.Th. Brinkman, R.J.J. Vreuls, At-line gas chromatographic–mass  
14 spectrometric analysis of fatty acid profiles of green microalgae using a direct thermal  
15 desorption interface, *Journal of Chromatography A* 959 (2002) 191–201.  
16 [https://doi.org/10.1016/S0021-9673\(02\)00463-6](https://doi.org/10.1016/S0021-9673(02)00463-6).
- 17 [139] R. Ishiwatari, S. Yamamoto, S. Shinoyama, Lignin and fatty acid records in Lake Baikal sediments  
18 over the last 130kyr: A comparison with pollen records, *Organic Geochemistry* 37 (2006) 1787–  
19 1802. <https://doi.org/10.1016/j.orggeochem.2006.10.005>.
- 20 [140] J.K. Volkman, Lipid Markers for Marine Organic Matter, in: J.K. Volkman (Ed.), *Marine Organic*  
21 *Matter: Biomarkers, Isotopes and DNA*, Springer, Berlin, Heidelberg, 2006: pp. 27–70.  
22 [https://doi.org/10.1007/698\\_2\\_002](https://doi.org/10.1007/698_2_002).
- 23 [141] P. Wen, Y. Wang, W. Huang, W. Wang, T. Chen, Z. Yu, Linking Microbial Community Succession  
24 With Substance Transformation in a Thermophilic Ectopic Fermentation System, *Front*  
25 *Microbiol* 13 (2022) 886161. <https://doi.org/10.3389/fmicb.2022.886161>.
- 26 [142] G. Kaur, B.W. Mountain, E.C. Hopmans, R.D. Pancost, Preservation of Microbial Lipids in  
27 Geothermal Sinters, *Astrobiology* 11 (2011) 259–274. <https://doi.org/10.1089/ast.2010.0540>.
- 28 [143] G. Kaur, B.W. Mountain, R.D. Pancost, Microbial membrane lipids in active and inactive sinters  
29 from Champagne Pool, New Zealand: Elucidating past geothermal chemistry and microbiology,  
30 *Organic Geochemistry* 39 (2008) 1024–1028.  
31 <https://doi.org/10.1016/j.orggeochem.2008.04.016>.
- 32 [144] G. Kaur, B.W. Mountain, M.B. Stott, E.C. Hopmans, R.D. Pancost, Temperature and pH control  
33 on lipid composition of silica sinters from diverse hot springs in the Taupo Volcanic Zone, New  
34 Zealand, *Extremophiles* 19 (2015) 327–344. <https://doi.org/10.1007/s00792-014-0719-9>.
- 35 [145] A. Weerkamp, W. Heinen, Effect of Temperature on the Fatty Acid Composition of the Extreme  
36 Thermophiles, *Bacillus caldolyticus* and *Bacillus caldotenax*, *Journal of Bacteriology* 109 (1972)  
37 443–446. <https://doi.org/10.1128/jb.109.1.443-446.1972>.
- 38 [146] C.E. Robertson, J.K. Harris, J.R. Spear, N.R. Pace, Phylogenetic diversity and ecology of  
39 environmental Archaea, *Current Opinion in Microbiology* 8 (2005) 638–642.  
40 <https://doi.org/10.1016/j.mib.2005.10.003>.
- 41 [147] D. Boulesteix, A. Buch, C. Szopa, Y. He, C. Freissinet, D. Coscia, Extremophile Metabolite Study  
42 to Detect Potential Biosignatures and Interpret Future Gas Chromatography-Mass  
43 spectrometry Ocean Worlds in situ analysis (e.g. Dragonfly mission with its DraMS instrument  
44 and EuropaLander with its EMILI instrument)., in: *AGU Fall Meeting Abstracts, 2022*: pp. P55G-  
45 1650.
- 46 [148] M.D. Giulio, The Universal Ancestor was a Thermophile or a Hyperthermophile: Tests and  
47 Further Evidence, *Journal of Theoretical Biology* 221 (2003) 425–436.  
48 <https://doi.org/10.1006/jtbi.2003.3197>.
- 49 [149] M.D. Cantine, G.P. Fournier, Environmental Adaptation from the Origin of Life to the Last  
50 Universal Common Ancestor, *Orig Life Evol Biosph* 48 (2018) 35–54.  
51 <https://doi.org/10.1007/s11084-017-9542-5>.

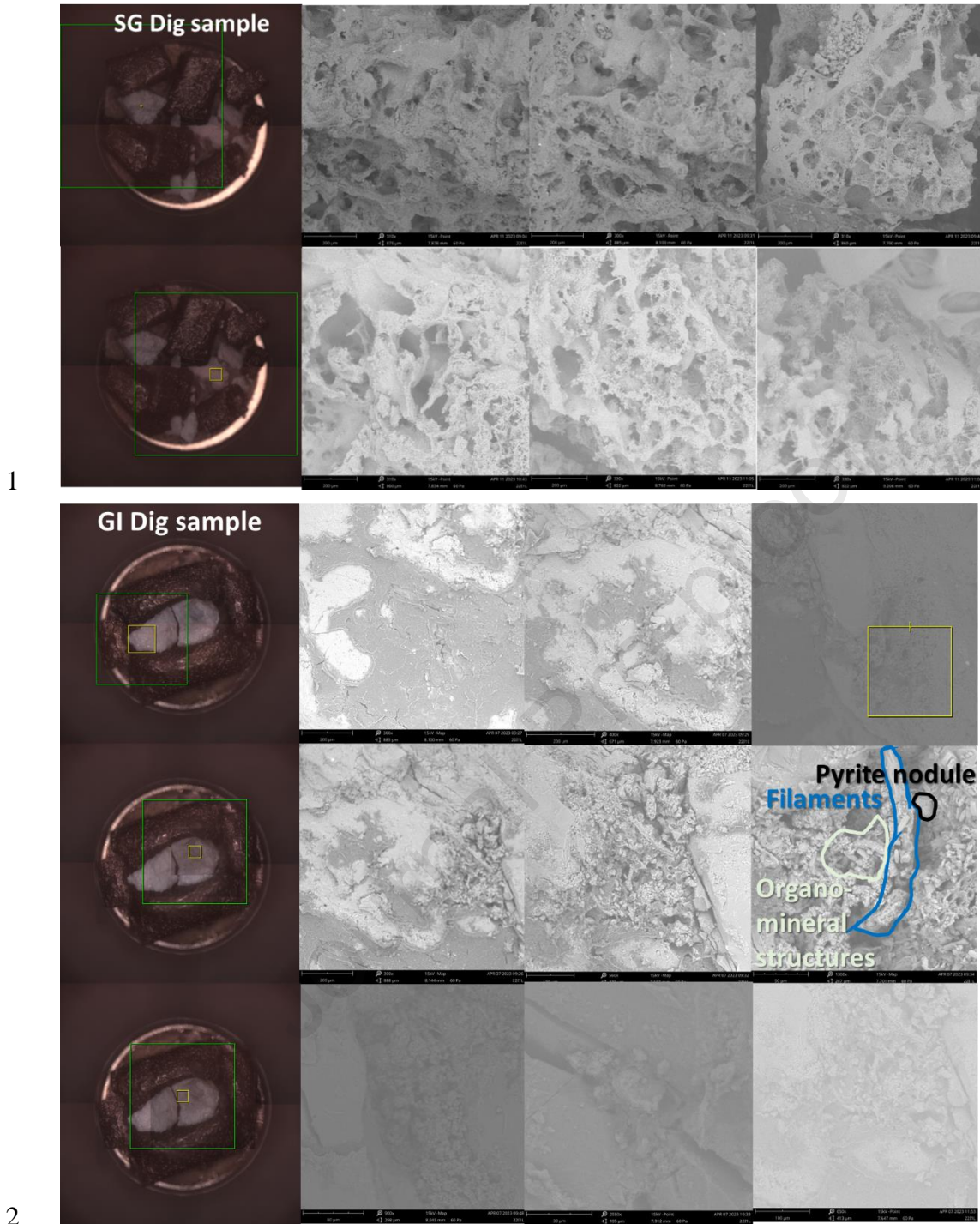
- 1 [150] J. Shiea, S.C. Brassel, D.M. Ward, Comparative analysis of extractable lipids in hot spring  
2 microbial mats and their component photosynthetic bacteria, *Organic Geochemistry* 17  
3 (1991) 309–319. [https://doi.org/10.1016/0146-6380\(91\)90094-Z](https://doi.org/10.1016/0146-6380(91)90094-Z).
- 4 [151] J.L. Harwood, N.J. Russell, Introduction, in: J.L. Harwood, N.J. Russell (Eds.), *Lipids in Plants*  
5 *and Microbes*, Springer Netherlands, Dordrecht, 1984: pp. 1–6. [https://doi.org/10.1007/978-](https://doi.org/10.1007/978-94-011-5989-0_1)  
6 [94-011-5989-0\\_1](https://doi.org/10.1007/978-94-011-5989-0_1).
- 7 [152] R.A. Gibson, A. Sherry, G. Kaur, R.D. Pancost, H.M. Talbot, Bacteriohopanepolyols preserved  
8 in silica sinters from Champagne Pool (New Zealand) indicate a declining temperature  
9 gradient over the lifetime of the vent, *Organic Geochemistry* 69 (2014) 61–69.  
10 <https://doi.org/10.1016/j.orggeochem.2014.02.004>.
- 11 [153] M. Ferrari, S. De Angelis, M.C. De Sanctis, A. Frigeri, F. Altieri, E. Ammannito, M. Formisano,  
12 V. Vinogradoff, Constraining the Rosalind Franklin Rover/Ma\_MISS Instrument Capability in  
13 the Detection of Organics, *Astrobiology* 23 (2023) 691–704.
- 14 [154] J.-P. Bibring, V. Hamm, C. Pilorget, J.L. Vago, The MicrOmega Investigation Onboard ExoMars,  
15 *Astrobiology* 17 (2017) 621–626. <https://doi.org/10.1089/ast.2016.1642>.
- 16 [155] M. Veneranda, G. Lopez-Reyes, J.A. Manrique-Martinez, A. Sanz-Arranz, J. Medina, C. Pérez,  
17 C. Quintana, A. Moral, J.A. Rodríguez, J. Zafra, L.M. Nieto Calzada, F. Rull, Raman  
18 spectroscopy and planetary exploration: Testing the ExoMars/RLS system at the Tabernas  
19 Desert (Spain), *Microchemical Journal* 165 (2021) 106149.  
20 <https://doi.org/10.1016/j.microc.2021.106149>.
- 21  
22  
23  
24  
25  
26  
27  
28  
29  
30  
31  
32  
33  
34  
35  
36  
37

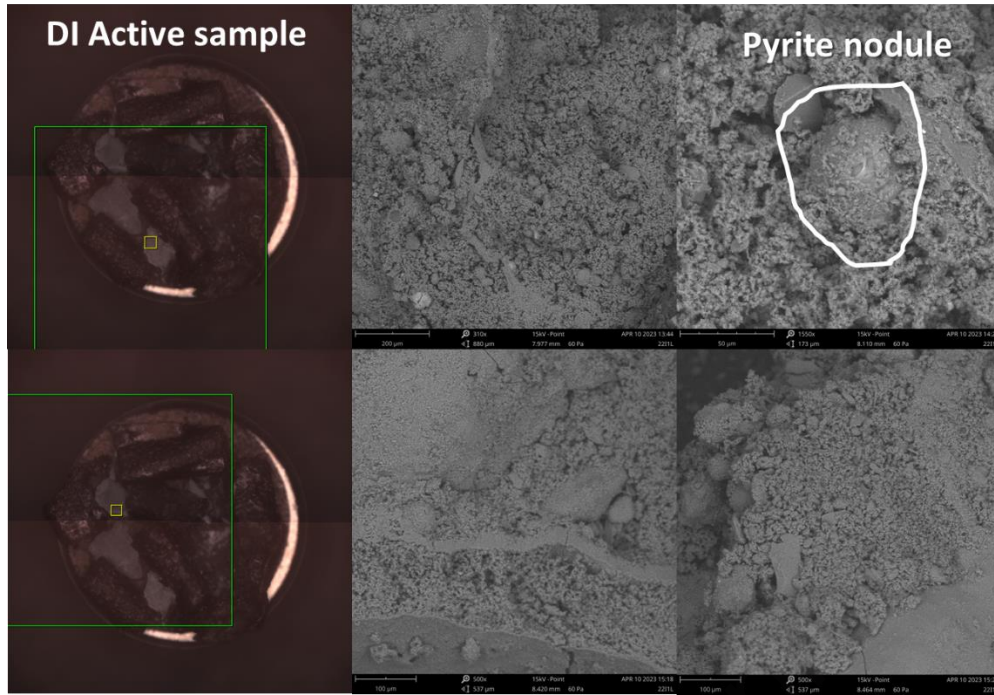
1 **Supplementary material**

2 **Supplementary material 1:** SEM-EDX mapping analysis on 'Goldilocks' : GI Dig (G1  
 3 sample) or SG Dig (S1 sample) to correlate with ICP-MS observations with averaged  
 4 percentages in elements on the mapping zone (yellow) followed by SEM pictures of  
 5 different features within the four different samples.

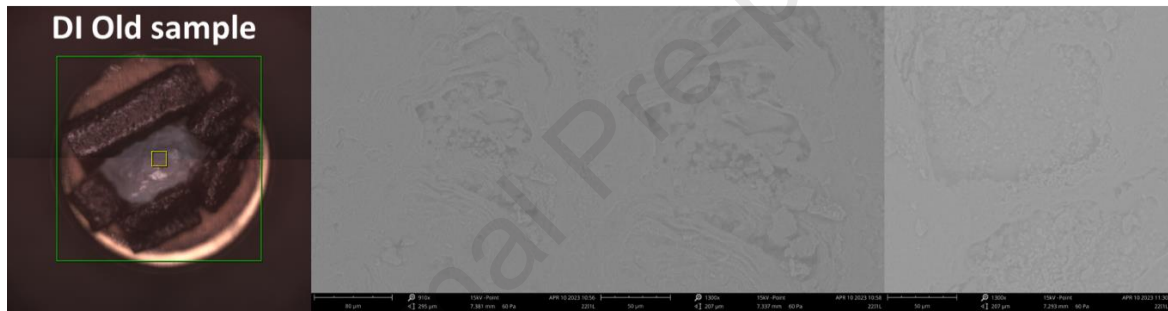


6



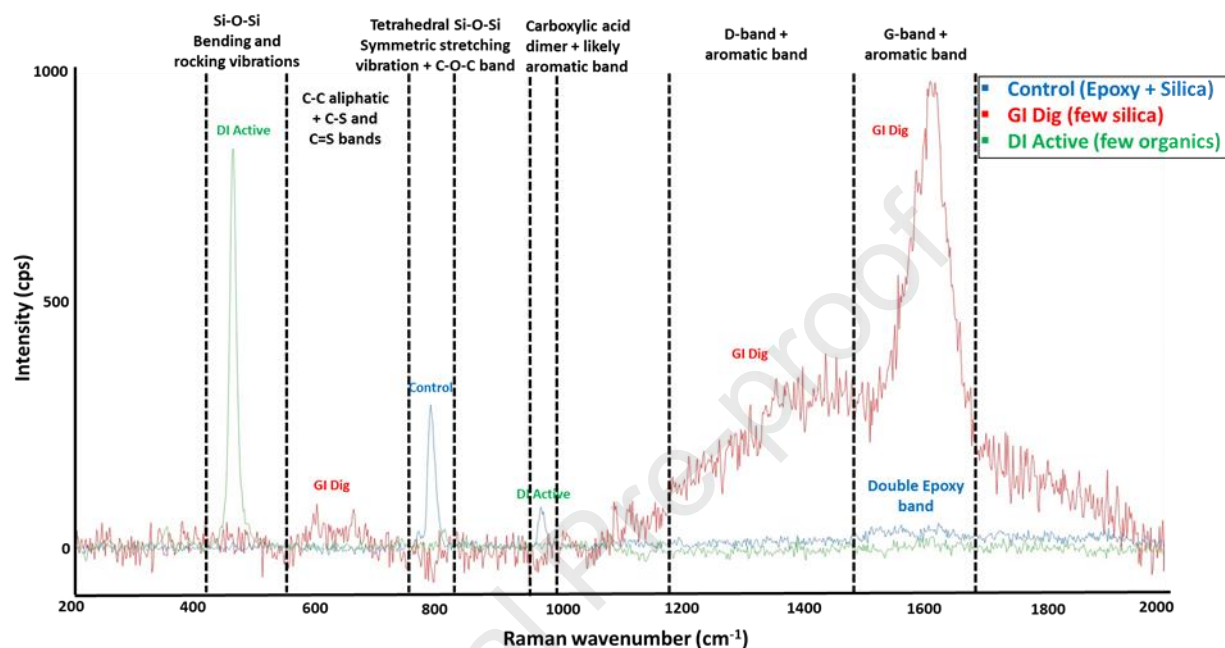


1



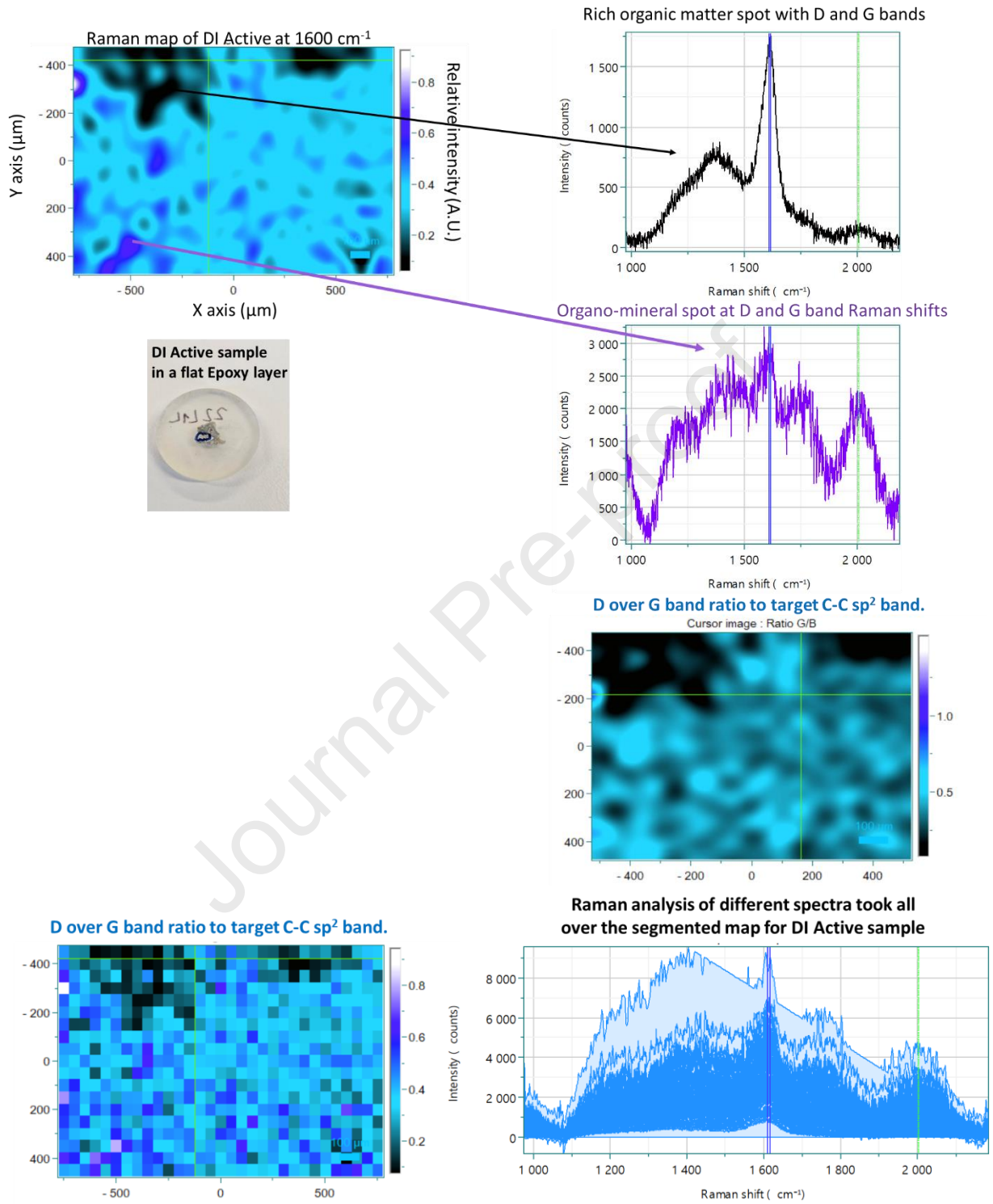
2  
3  
4  
5  
6  
7  
8  
9  
10  
11  
12  
13  
14  
15  
16  
17  
18  
19  
20  
21  
22  
23  
24  
25

1 **Supplementary material 2:** Raman analysis of the Epoxy matrix thin layer on the top  
 2 of the siliceous sinter sample (a) and a piece of sample arisen on the surface of the  
 3 Epoxy matrix with the observation of organic matter (b) G-bands different from the  
 4 Epoxy double-bond (excitation source at 325 nm). We focused for DI Active and SG  
 5 Dig samples on the D and G band region since these samples presented less organic  
 6 matter diversity according to mass spectrometry analysis (than GI Dig) and we did not  
 7 observe the D band for DI Active sample.



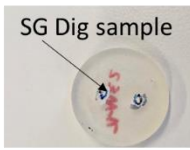
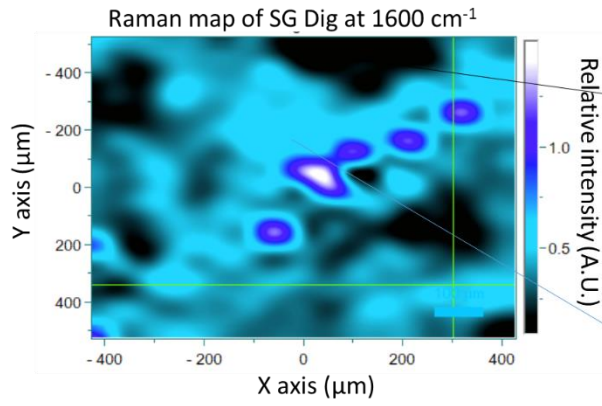
8  
9  
10  
11  
12  
13  
14  
15  
16  
17  
18  
19  
20  
21  
22  
23  
24  
25  
26  
27  
28  
29  
30  
31

- 1 Raman analysis on DI Old and SG Dig with the OM in the amorphous silica matrix (black curves) and the
- 2 Epoxy and silica matrix (purple/blue curves).

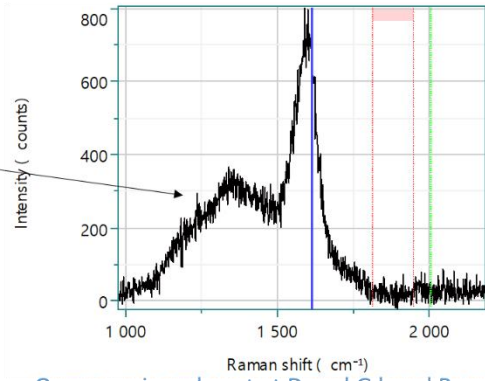


3

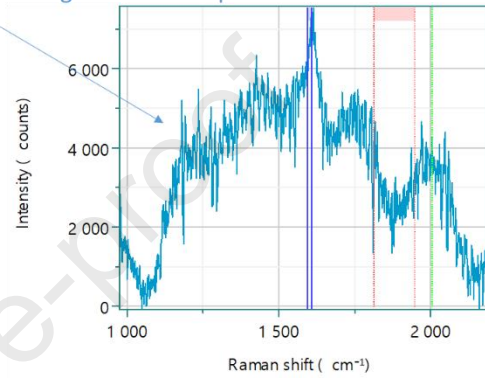
4



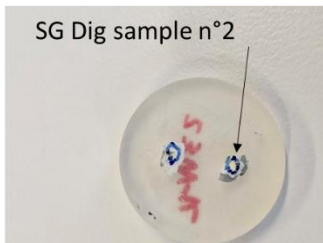
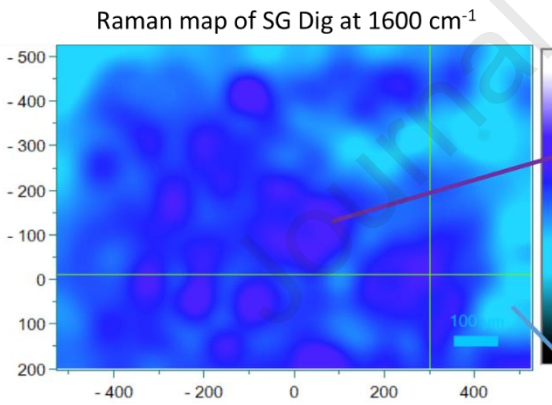
Rich organic matter spot with D and G bands



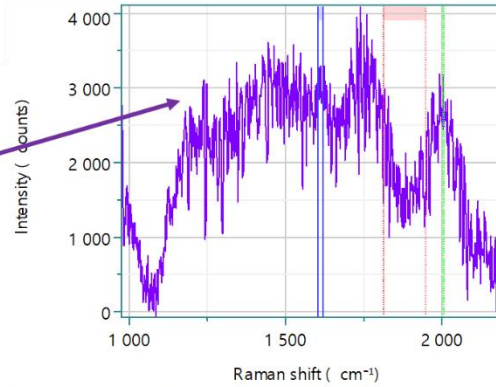
Organo-mineral spot at D and G band Raman shifts



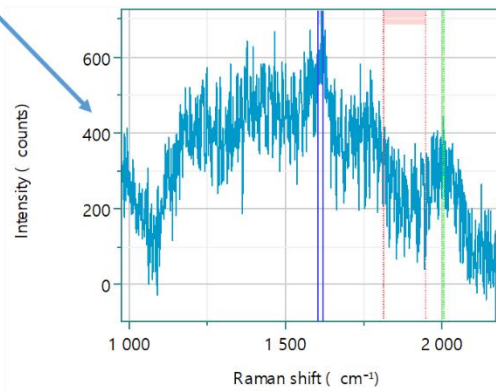
1



Slightly richer organic matter spot

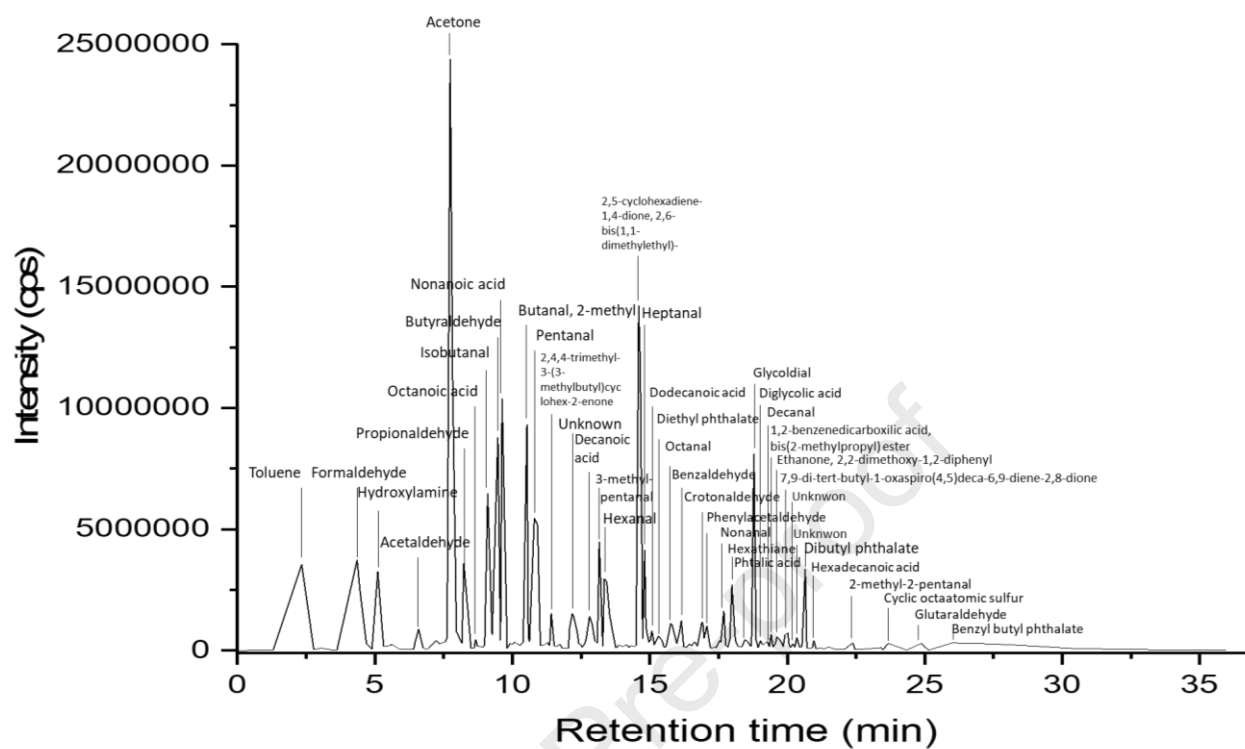


Organo-mineral spot at D and G band Raman shifts



2  
3  
4  
5

- 1 **Supplementary material 3:** Total Ion Chromatograms of PFBHA SPME-GC-MS  
 2 analysis on GI Dig (modern “Goldilocks” – Sylvan spring siliceous sinter).



- 3  
4

### Highlights

- The spaceflight untargeted metabolomics method successfully identified biosignatures.
- The Mars GC-MS sample processes enable bioindicator and biosignature differentiation.
- Yellowstone hot springs are relevant analog to Mars volcanic/crater systems.
- Temperature and pH drive together biosignature preservation and microbial diversity.
- Biosignature detection on Mars would be revealed by a set of geo-chemical features.

Journal Pre-proof

**Declaration of interests**

The authors declare that they have no known competing financial interests or personal relationships that could have appeared to influence the work reported in this paper.

The authors declare the following financial interests/personal relationships which may be considered as potential competing interests:

Boulesteix David reports travel was provided by Fulbright. Boulesteix David reports a relationship with CentraleSupélec that includes: funding grants. If there are other authors, they declare that they have no known competing financial interests or personal relationships that could have appeared to influence the work reported in this paper.